tramembrane proteolysis of HCV core protein signal sequence of genotypes 1a and 1b by SPP.

To further examine the cleavage of the signal sequence of HCV core proteins by SPP, we prepared IF176/177AL and the spmt mutant core proteins carrying a substitution of Ala^{191} to Arg to avoid processing by signal peptidase as described above. In cells expressing a wild-type or LVL/3A mutant core protein, a 23-kDa processed or a 25-kDa unprocessed core protein was detected, as seen in Fig. 3B (Fig. 4D, lanes 2 and 4). The IF176/177AL mutant exhibited a 26-kDa unprocessed band which was detected by anti-HA antibody (Fig. 4D, lane 5). In contrast, the spmt core protein exhibited a major band at 23 kDa and a faint 24-kDa band after blotting with the anti-Flag antibody (Fig. 4D, lane 3). Detection of a small amount of the 24-kDa unprocessed band by the anti-HA antibody indicates that most of the spmt mutant core protein was processed by SPP. The unprocessed core proteins of spmt, LVL/3A and IF176/177AL exhibited different electrophoretic mobilities, estimated to be 24, 25, and 26 kDa, respectively (Fig. 4D, lower panel, lanes 3 to 5). Lemberg and Martoglio pointed out that the mobility of a protein does not necessarily correlate with its molecular mass when analyzed in a Tris-glycine gel system due to the unexpected electrophoretic mobility of the proteins (22). However, detection of HA-tagged unprocessed signal sequence in the core mutants clearly demonstrated that LVL/3A and IF176/177AL mutants substituted with Leu^{139}, Val^{140}, and Leu^{144} in domain 2 and with Ile^{176} and Phe^{177} in the transmembrane domain, respectively, have lost the ability to be cleaved by SPP.

Effect of a loss-of-function mutant of SPP on the processing of the signal sequence of HCV core protein. Although there are two reports suggesting that SPP is involved in the processing of the signal sequence of HCV core protein by using the SPP inhibitor $(Z\text{-}LL)_2$-keton (23, 30), a direct interaction of HCV core protein with SPP has not been demonstrated. To determine the direct involvement of SPP in the processing of HCV core protein signal sequence, the C-terminal HA tag in the Flag-Core-E1-HA constructs used in the experiments described above was replaced with a myc/His tag and coexpressed with wild-type SPP (SPP-HAER) or with a mutant SPP with amino acid substitutions in the putative protease active sites, i.e., Asp^{219} (SPP D219A-HAER) or Asp^{265} (SPP D265A-HAER) to Ala. The signal sequence of HCV core protein was processed in cells coexpressing Flag-Core-E1-myc/His and SPP-HAER (Fig. 5, anti-Flag, lane 3), whereas two bands corresponding to processed and unprocessed (the same size as Flag-Core LVL/3A-E1-myc/His [lane 6]) core proteins were detected in cells coexpressing Flag-Core-E1-myc/His and the mutant SPP constructs (Fig. 5, anti-Flag, lanes 4 and 5). Proper cleavage and glycosylation of E1 proteins in cells coexpressing Flag-Core-E1-myc/His and the SPP mutants (Fig. 5, anti-His, lanes 4 and 5) and those expressing Flag-Core LVL/3A-E1-myc/His (Fig. 5, anti-His, lane 6) indicates that processing of signal sequence by SPP is not required for the cleavage of the core-E1 junction by signal peptidase and translocation of E1 protein into the ER. These results indicate that loss-of-function mutants of SPP inhibit the intramembrane proteolysis of HCV core protein signal sequence and further confirm that the slightly larger bands detected in cells expressing Flag-Core

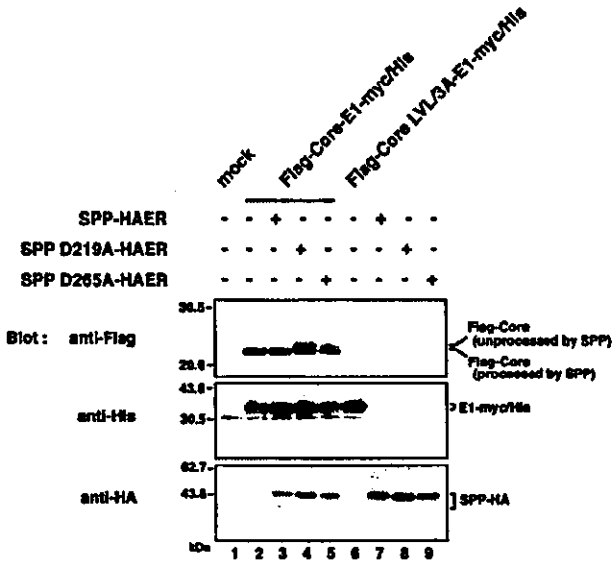

FIG. 5. Effect of loss-of-function mutants of SPP on the processing of the signal sequence of HCV core protein. SPP-HAER, SPPD219A-HAER, or SPPD265A-HAER was coexpressed with Flag-Core-E1-myc/His or Flag-Core LVL/3A-E1-myc/His in 293T cells. Cell lysates were analyzed by immunoblotting with anti-Flag (upper panel), anti-His_6 (middle panel), or anti-HA (lower panel) antibody. + and −, presence or absence of each plasmid, respectively. Lane 1, mock; lanes 2, 6, 7, 8, and 9, single expression of Flag-Core-E1-myc/His, Flag-Core LVL/3A-E1-myc/His, SPP-HAER, SPPD219A-HAER, and SPPD265A-HAER, respectively; lanes 3 to 5, coexpression of Flag-Core-E1-myc/His with SPP-HAER, SPPD219A-HAER, and SPPD265A-HAER, respectively.

LVL/3A-E1-HA or Flag-Core IF176/177AL-E1-HA are immature core proteins unprocessed by SPP (Fig. 4B, lanes 3 and 9).

Interaction of HCV core protein with SPP. To examine the specific interaction of HCV core protein with SPP, Flag-Core-E1-myc/His, Flag-Core LVL/3A-E1-myc/His, or Flag-Core IF176/177AL-E1-myc/His was coexpressed with SPP-HAER or SPP D219A-HAER in 293T cells and immunoprecipitated with anti-Flag or anti-HA antibody. In cells coexpressing the loss-of-function mutant, SPP D219A-HAER, and one of the three HCV polyprotein substrates, nonspecific bands were detected by immunoblotting with the anti-HA and anti-Flag antibodies in the immunoprecipitates (Fig. 6A, upper and second panels, lanes 3 to 5). Therefore, lysates immunoprecipitated with anti-Flag and anti-HA antibodies were evaluated by comparison with those precipitated with anti-EE. Three bands corresponding to SPP D219A-HAER were coimmunoprecipitated with core proteins by anti-Flag immunoprecipitation (Fig. 6A, upper panel, lanes 8 to 10). SPP has two glycosylation sites (50), and therefore the upper, middle, and lower bands seem to correspond to SPP possessing two glycans, one glycan, and no glycan, respectively. Deglycosylation by PNGase F treatment reduced the molecular sizes of all bands to that of the lowest band (data not shown). Only unprocessed core protein was coimmunoprecipitated with SPP D219A-HAER by anti-HA (Fig. 6A, second panel, lanes 8 to 10). Coexpression of Flag-Core LVL/3A-E1-myc/His or Flag-Core-IF176/177AL-E1-myc/His reduced the expression of SPP D219A-HAER (Fig. 6A, third panel, lanes 4 and 5), suggesting that the

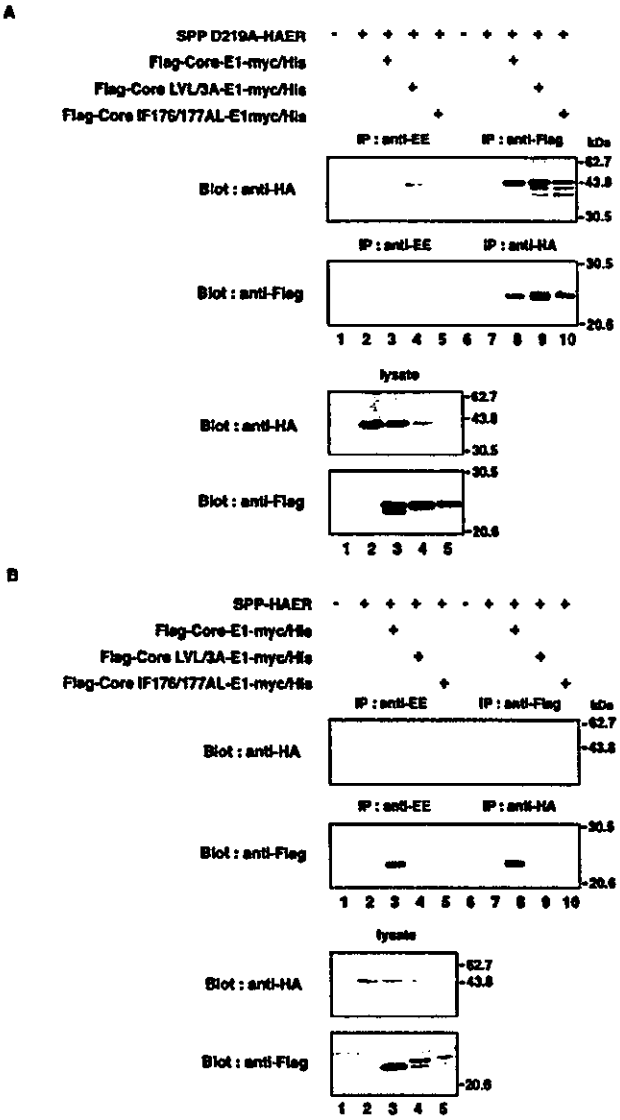

FIG. 6. Interaction of HCV core protein with SPP. SPP D219A-HAER (A) or SPP-HAER (B) was coexpressed with Flag-Core-E1-myc/His, Flag-Core LVL/3A-E1-myc/His, or Flag-Core IF176/177AL-E1-myc/His in 293T cells and immunoprecipitated (IP) with anti-Flag or anti-HA antibody. The immunoprecipitates were analyzed by immunoblotting with anti-HA or anti-Flag antibody. As a control, immunoprecipitation was carried out with anti-EE antibody. + and −, presence or absence of each plasmid, respectively.

core mutants suppress the expression of the SPP mutant. Clear reduction or elimination of the processing of the HCV core protein signal sequence was observed in cells coexpressing SPP D219A-HAER in comparison with those coexpressing wild-type SPP (Fig. 6A and B, bottom panels, lanes 3 to 5). Conversely, no interaction of HCV core protein with wild-type SPP was observed in cells coexpressing SPP-HAER and the HCV polyprotein substrates (Fig. 6B, upper panels, lanes 8 to 10). Broad bands were detected in immunoprecipitates with anti-Flag or anti-EE antibody by immunoblotting with the anti-Flag antibody, probably due to nonspecific binding of the processed

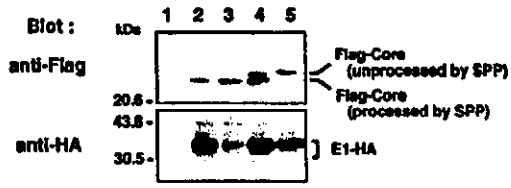

FIG. 7. Processing of HCV core-E1 polyprotein in the human hepatoma cell line FLC-4. Flag-Core-E1-HA (lane 2), Flag-Core ASC/VLV-E1-HA (lane 3), Flag-Core LVL/3A-E1-HA (lane 4), or Flag-Core IF176/177AL-E1-HA (lane 5) was expressed in FLC-4 cells and analyzed by immunoblotting with anti-Flag (upper panel) or anti-HA (lower panel) antibody. Cells transfected with an empty plasmid were used as a negative control (lane 1).

core protein to protein G-Sepharose (Fig. 6B, second panel, lanes 3 and 8). These results indicate that a direct interaction of SPP with HCV core protein only between the unprocessed core protein and the loss-of-function mutant of SPP is verifiable. SPP should bind to the signal sequence of HCV core protein and release it after proteolysis, whereas SPP D219A cannot liberate the substrate after binding due to lack of the catalytic activity, suggesting that the SPP mutant may possess dominant negative effects.

Processing of the signal sequence of HCV polyprotein in a human hepatoma cell line. To confirm the data obtained for 293T cells with human liver cells, processing of core-E1 polyprotein in FLC4 cells, a human hepatoma cell line, was examined (Fig. 7). Processing by signal peptidase and SPP was evident in cells expressing Flag-Core-E1-HA or Flag-Core ASC/VLV-E1-HA (lanes 2 and 3), whereas clear processing by signal peptidase, but not complete cleavage by SPP, was observed in FLC-4 cells expressing Flag-Core LVL/3A-E1-HA or Flag-Core IF176/177AL-E1-HA (lanes 4 and 5). These results are consistent with data obtained with 293T cells, suggesting that the processing of the signal sequence of HCV core protein is not cell type dependent or an artifact of the techniques used in this study.

Localization of mutant HCV core proteins. To determine the effect of mutations on the localization of HCV core protein, EGFP-Core 191and its mutants that are defective in cleavage by SPP were expressed in HeLa cells (Fig. 8A). EGFP-Core 191 was processed by SPP and colocalized with an ER marker. EGFP-Core IF176/177AL, which bears a mutation that confers α-helix structure to the signal sequences, was diffusely distributed but did not completely colocalize with ER-DsRed as seen with EGFP-Core 191. EGFP-Core LVL/3A was localized mainly to the nucleus and, to a lesser extent, the cytoplasm, and EGFP-Core Δ128-151 exhibited complete nuclear localization. To confirm the subcellular localization of mutant HCV core proteins, cells were transfected with expression plasmids encoding N-terminally Flag-tagged and C-terminally HA-tagged core proteins to minimize the effect of fusion protein and fractionated, as described in Materials and Methods (Fig. 8B). Consistent with the subcellular localization of EGFP-Core proteins, Flag-Core 191-HA was detected mainly in the membrane-organelle fraction and Flag-Core LVL/3A-HA and Flag-Core Δ128-151-HA were localized mainly in the nuclear fraction. Although EGFP-Core IF176/177AL did not completely colocalize with the ER marker, 55% of Flag-

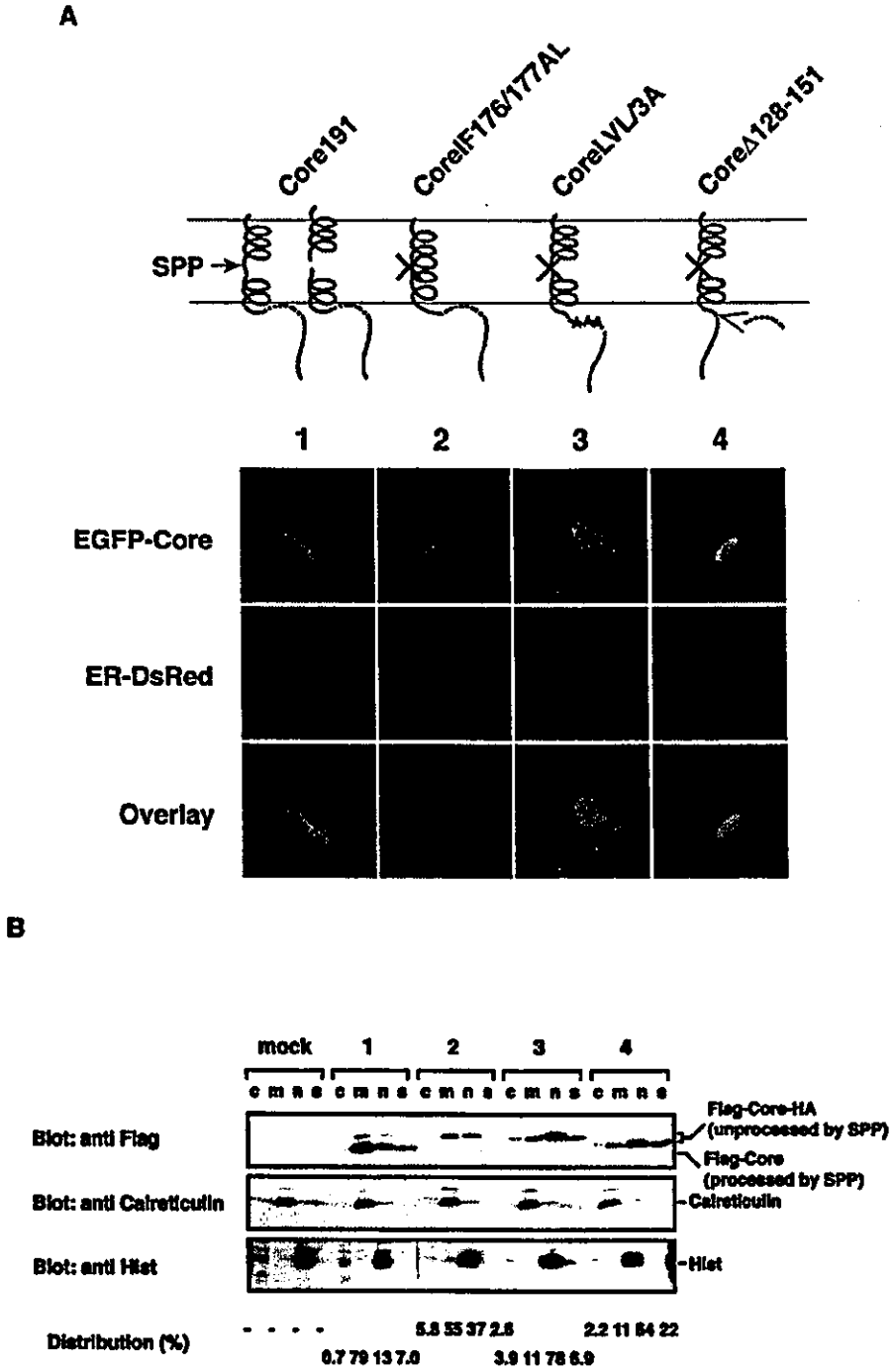

FIG. 8. Localization of mutant HCV core proteins. (A) Putative processing mechanisms of wild-type and mutant core proteins is illustrated at the top. EGFP-Core-191 (column 1), EGFP-Core IF176/177AL (column 2), EGFP-Core LVL/3A (column 3), and EGFP-Core Δ128-151 (column 4) were coexpressed with ER-DsRed in HeLa cells, and subcellular localization of core proteins was examined by confocal microscopy. (B) Subcellular fractionation of HeLa cells transfected with plasmids encoding Flag-Core-HA polyproteins. Cells transfected with an empty plasmid (lane M) or plasmid encoding Flag-Core 191-HA (lanes 1), Flag-Core IF176/177AL-HA (lanes 2), Flag-Core LVL/3A-HA (lanes 3), or Flag-Core Δ128-151-HA (lanes 4) were extracted into four fractions, as described in Materials and Methods. Each fraction was concentrated and subjected to immunoblotting with anti-Flag antibody (upper panel). Lanes c, m, n and s, cytosol, membrane-organelle, nuclear, and cytoskeleton fractions, respectively. Calreticulin and histone (His) were used as markers for membrane-organelle and nuclear fractions, respectively. To determine the distributed ratio of processed and unprocessed core proteins in each fraction, the density of core protein in each fraction was measured and is indicated as a percentage at each bottom of lane.

Core IF176/177AL-HA was detected in membrane-organelle fraction. Since we could not separate ER and Golgi fractions by the fractionation method used, it is possible that Flag-Core IF176/177AL-HA localizes mainly in the Golgi rather than the ER. These results indicate that not only the C-terminal signal sequence but also the hydrophobic region from amino acid 139 to 144 in domain 2 and proper processing by SPP are involved in the ER retention of HCV core protein.

DISCUSSION

Hope and McLauchlan identified three regions in the HCV core protein, including two hydrophobic regions in the C-terminal one-third of the protein and the region from amino acid 119 to 174, which was designated domain 2 (12). Domain 2 was hypothesized to interact with lipid droplets and confer stability to the HCV core protein (12). Although a mutation in the signal sequence of core protein that renders it resistant to SPP proteolysis restored retention on lipid droplets and overall stability (30), deletion of domain 2 from HCV core protein leads to diffusion in the cytoplasm and degradation after processing by signal peptidase (30). Indeed, these data suggest that mature HCV core protein is retained on lipid droplets via domain 2, but they do not necessarily indicate that the region is required for the ER retention of HCV core protein. The intramembrane proteolysis of the signal sequence of HCV core protein by SPP is abolished when helix-breaking and -bending residues in the C-terminal signal-anchor sequence are replaced by basic amino acids (30). However, the involvement of other regions of HCV core protein in processing by SPP is not known. In this study, we could demonstrate that not only the C-terminal signal-anchor domain but also three hydrophobic amino acids Leu^{139}, Val^{140}, and Leu^{144} in domain 2 are required for intramembrane proteolysis by SPP. However, this domain is not essential for the cleavage of the core-E1 junction by signal peptidase or for translocation of E1 into the ER. Furthermore, the nuclear localization of domain 2 core mutants possessing an unprocessed C-terminal signal-anchor sequence indicates that association with the ER membrane through domain 2 is required for ER retention of HCV core protein.

Martoglio and colleagues demonstrated, by using a Semliki Forest virus expression system, that Ala^{180}, Ser^{183}, and Cys^{184} break the α-helical structure within the signal sequence and are essential for the intramembrane proteolysis of HCV core protein of the type 1a Glasgow strain by SPP in BHK and Huh7 cell lines (23, 30). However, mutation of Ala^{180}, Ser^{183}, and Cys^{184} in core proteins of the type 1b J1 and type 1a H77 strains could not inhibit signal sequence processing by SPP in the BHK and 293T cell lines by expression with plasmid. HCV core protein of the type 1a Glasgow strain shares 96.3 and 95.8% amino acid homology to those of the H77c and J1 strains, respectively. Furthermore, the signal sequences of the core proteins of these three strains are almost identical, and therefore the observed differences in cleavability by SPP might be attributable to sequence other than the signal sequence or expression system used. We reexamined the HCV core protein signal sequence and, using the method of Garnier et al. (9), chose to further examine Ile^{176} and Phe^{177} as residues that may interfere with the assumption of a compact α-helix structure and allow for intramembrane proteolysis by SPP. Mutation of Ile^{176} and Phe^{177} (Core IF176/177AL) of genotype 1a and 1b strains, which is predicted to confer α-helical structure to the signal sequences, inhibited processing by SPP. EGFP-Core IF176/177AL exhibited no colocalization with an ER marker; this differs from the case for the wild-type core protein. These data suggest that the processing of the signal sequence by SPP may play a role in the ER retention of HCV core protein.

Precursor HCV core protein consists of 191 amino acids and is processed by signal peptidase from a polyprotein after translocation of the C-terminal signal-anchor sequence into the ER. This is then cleaved by SPP into the mature core protein and localizes primarily to the ER. The mature core protein, further processed by an unidentified protease, is composed of amino acids 151 to 153 and is detected in the nucleus (33, 47). Actually, HCV core protein is observed in the cytoplasm, nucleus, and nucleoli in transgenic mice expressing HCV core protein (35). Under normal conditions, the precursor core protein is processed by SPP to 173 to 179 amino acids and localizes to the ER. In contrast, a 179-amino-acid construct containing a limited C-terminal anchor-signal sequence, Core 179, localizes primarily to the nucleus and to the ER to a lesser extent. This striking difference in the subcellular localizations of Core 191 and Core 179, in conjunction with data from the Core IF176/177AL construct, indicates that the presence of the full-length signal-anchor sequence and proper processing by SPP is required for retention of HCV core protein on the ER membrane.

We also demonstrated that the reduction in hydrophobicity in domain 2 affects proteolysis of the signal sequence by SPP and localization of HCV core protein. It was suggested that HCV core protein interacts with lipid droplets containing triacylglycerol and/or ER membrane through domain 2 irrespective of intramembrane proteolysis of the signal sequence (30). A mutant HCV core protein in domain 2, EGFP-Core LVL/3A with Leu^{139}, Val^{140}, and Leu^{144} replaced by Ala, was processed by signal peptidase but not by SPP and localized to the nucleus in spite of the presence of an unprocessed hydrophobic signal sequence in the C terminus. This result suggests that penetration of the HCV core protein signal sequence into the ER membrane is necessary, but not sufficient, for ER retention of HCV core protein. Insertion of the C-terminal signal-anchor sequence of core protein into the ER may induce conformational changes in domain 2 to render it accessible to the ER membrane and/or lipid droplets by exposure of hydrophobic residues in the domain, residues that are well conserved among various genotypes of HCV. Although it was suggested that processed HCV core protein was retained on the ER membrane via an interaction with unprocessed core protein (25) or with the C-terminal transmembrane region of E1 (26), our data provide a new model of the ER retention of HCV core protein. HCV core protein is a structural protein that forms the nucleocapsid, and virus particles are thought to be released into ER. Therefore, retention of HCV core protein on the ER membrane should be essential for the assembly of HCV.

Intramembrane-cleaving proteases have been shown to play pivotal roles in cell regulation and signaling and are involved in diseases such as Alzheimer's disease (52). SPP belongs to a family of aspartic proteases family and has two aspartic acid residues, Asp^{219} and Asp^{265}, in the enzyme active site (50).

Signal peptidase II also belongs to this aspartic protease family and cleaves the signal sequence by attacking a proton of a water molecule via an aspartic acid of the enzyme (38). Mutant SPP bearing an Asp^{265}-to-Ala substitution was deficient in the processing of HLA-A but retained binding activity to the SPP substrate analogue TBL_4K (50). We could demonstrate a direct interaction by immunoprecipitation of unprocessed HCV core proteins with mutant SPP lacking catalytic and substrate-releasing activities by replacement of Asp^{219} with Ala. Binding of the loss-of-function SPP mutants with unprocessed core proteins irrespective of mutation or deletion in domain 2 indicates that the domain is not directly involved in the interaction.

It has been demonstrated that expression of HCV core protein alone is sufficient for the induction of hepatic steatosis and hepatocellular carcinoma in transgenic mice (24, 34, 35). Furthermore, we demonstrated that nuclear localization and degradation of HCV core protein is regulated by PA28γ-dependent proteolysis (33). These findings suggest that HCV core protein plays a pivotal role in the development of hepatocellular carcinoma and that intramembrane proteolysis may regulate the subcellular localization of HCV core protein. Although the SPP inhibitor $(Z\text{-}LL)_2$-keton suppresses cleavage of signal sequence essential for homeostasis, host defense, etc., a specific inhibitor against the intramembrane proteolysis of HCV core protein, such as antagonists for the binding of HCV core protein to ER membrane via domain 2, will be an effective antiviral drug for patients with chronic hepatitis C. Furthermore, involvement of intramembrane proteolysis by SPP in the processing of other HCV proteins and the fates of the peptides cleaved by SPP in the replication and pathogenesis of hepatitis C are subjects of future studies.

ACKNOWLEDGMENTS

We gratefully thank T. Shioda for advice on confocal microscopy and J. McLauchlan for valuable discussions.

This work was supported in part by grants-in-aid from the Ministry of Health, Labor and Welfare; the program for Promotion of Fundamental Studies in Health Sciences of the Organization for Drug ADR Relief, R&D Promotion, and Product Review; the Ministry of Education, Culture, Sports, Science and Technology; and the 21st Century Center of Excellence Program of Japan.

REFERENCES

1. **Aizaki, H., Y. Aoki, T. Harada, K. Ishii, T. Suzuki, S. Nagamori, G. Toda, Y. Matsuura, and T. Miyamura.** 1998. Full-length complementary DNA of hepatitis C virus genome from an infectious blood sample. Hepatology 27: 621–627.
2. **Bukh, J., R. H. Purcell, and R. H. Miller.** 1994. Sequence analysis of the core gene of 14 hepatitis C virus genotypes. Proc. Natl. Acad. Sci. USA 91:8239–8243.
3. **Chang, S. C., J. H. Yen, H. Y. Kang, M. H. Jang, and M. F. Chang.** 1994. Nuclear localization signals in the core protein of hepatitis C virus. Biochem. Biophys. Res. Commun. 205:1284–1290.
4. **Chen, C. M., L. R. You, L. H. Hwang, and Y. H. Lee.** 1997. Direct interaction of hepatitis C virus core protein with the cellular lymphotoxin-beta receptor modulates the signal pathway of the lymphotoxin-beta receptor. J. Virol. 71:9417–9426.
5. **Choo, Q. L., G. Kuo, A. J. Weiner, L. R. Overby, D. W. Bradley, and M. Houghton.** 1989. Isolation of a cDNA clone derived from a blood-borne non-A, non-B viral hepatitis genome. Science 244:359–362.
6. **Choo, Q. L., K. H. Richman, J. H. Han, K. Berger, C. Lee, C. Dong, C. Gallegos, D. Coit, R. Medina-Selby, P. J. Barr, A. J. Weiner, D. W. Bradley, G. Kuo, and M. Houghton.** 1991. Genetic organization and diversity of the hepatitis C virus. Proc. Natl. Acad. Sci. USA 88:2451–2455.
7. **Dubuisson, J., S. Duvet, J. C. Meunier, A. Op De Beeck, R. Cacan, C. Wychowski, and L. Cocquerel.** 2000. Glycosylation of the hepatitis C virus envelope protein E1 is dependent on the presence of a downstream sequence on the viral polyprotein. J. Biol. Chem. 275:30605–30609.
8. **Fliegel, L., K. Burns, D. H. MacLennan, R. A. Reithmeier, and M. Michalak.** 1989. Molecular cloning of the high affinity calcium-binding protein (calreticulin) of skeletal muscle sarcoplasmic reticulum. J. Biol. Chem. 264:21522–21528.
9. **Garnier, J., J. F. Gibrat, and B. Robson.** 1996. GOR method for predicting protein secondary structure from amino acid sequence. Methods Enzymol. 266:540–553.
10. **Grakoui, A., D. W. McCourt, C. Wychowski, S. M. Feinstone, and C. M. Rice.** 1993. Characterization of the hepatitis C virus-encoded serine proteinase: determination of proteinase-dependent polyprotein cleavage sites. J. Virol. 67:2832–2843.
11. **Ho, S. N., H. D. Hunt, R. M. Horton, J. K. Pullen, and L. R. Pease.** 1989. Site-directed mutagenesis by overlap extension using the polymerase chain reaction. Gene 77:51–59.
12. **Hope, R. G., and J. McLauchlan.** 2000. Sequence motifs required for lipid droplet association and protein stability are unique to the hepatitis C virus core protein. J. Gen. Virol. 81:1913–1925.
13. **Hope, R. G., D. J. Murphy, and J. McLauchlan.** 2002. The domains required to direct core proteins of hepatitis C virus and GB virus-B to lipid droplets share common features with plant oleosin proteins. J. Biol. Chem. 277:4261–4270.
14. **Horton, R. M., H. D. Hunt, S. N. Ho, J. K. Pullen, and L. R. Pease.** 1989. Engineering hybrid genes without the use of restriction enzymes: gene splicing by overlap extension. Gene 77:61–68.
15. **Houghton, M., A. Weiner, J. Han, G. Kuo, and Q. L. Choo.** 1991. Molecular biology of the hepatitis C viruses: implications for diagnosis, development and control of viral disease. Hepatology 14:381–388.
16. **Hussy, P., H. Langen, J. Mous, and H. Jacobsen.** 1996. Hepatitis C virus core protein: carboxy-terminal boundaries of two processed species suggest cleavage by a signal peptide peptidase. Virology 224:93–104.
17. **Kato, N., M. Hijikata, Y. Ootsuyama, M. Nakagawa, S. Ohkoshi, T. Sugimura, and K. Shimotohno.** 1990. Molecular cloning of the human hepatitis C virus genome from Japanese patients with non-A, non-B hepatitis. Proc. Natl. Acad. Sci. USA 87:9524–9528.
18. **Kiyosawa, K., T. Sodeyama, E. Tanaka, Y. Gibo, K. Yoshizawa, Y. Nakano, S. Furuta, Y. Akahane, K. Nishioka, R. H. Purcell, and H. J. Alter.** 1990. Interrelationship of blood transfusion, non-A, non-B hepatitis and hepatocellular carcinoma: analysis by detection of antibody to hepatitis C virus. Hepatology 12:671–675.
19. **Kuo, G., Q. L. Choo, H. J. Alter, G. L. Gitnick, A. G. Redeker, R. H. Purcell, T. Miyamura, J. L. Dienstag, M. J. Alter, C. E. Stevens, M. J. Alter, C. E. Stevens, G. E. Tegtmeier, F. Bonino, M. Colombo, W. S. Lee, C. Kuo, K. Berger, J. R. Shuster, L. R. Overby, D. W. Bradley, and M. Houghton.** 1989. An assay for circulating antibodies to a major etiologic virus of human non-A, non-B hepatitis. Science 244:362–364.
20. **Kyte, J., and R. F. Doolittle.** 1982. A simple method for displaying the hydropathic character of a protein. J. Mol. Biol. 157:105–132.
21. **Lemberg, M. K., F. A. Bland, A. Weihofen, V. M. Braud, and B. Martoglio.** 2001. Intramembrane proteolysis of signal peptides: an essential step in the generation of HLA-E epitopes. J. Immunol. 167:6441–6446.
22. **Lemberg, M. K., and B. Martoglio.** 2003. Analysis of polypeptides by sodium dodecyl sulfate-polyacrylamide gel electrophoresis alongside in vitro-generated reference peptides. Anal. Biochem. 319:327–331.
23. **Lemberg, M. K., and B. Martoglio.** 2002. Requirements for signal peptide peptidase-catalyzed intramembrane proteolysis. Mol. Cell 10:735–744.
24. **Lerat, H., M. Honda, M. R. Beard, K. Loesch, J. Sun, Y. Yang, M. Okuda, R. Gosert, S. Y. Xiao, S. A. Weinman, and S. M. Lemon.** 2002. Steatosis and liver cancer in transgenic mice expressing the structural and nonstructural proteins of hepatitis C virus. Gastroenterology 122:352–365.
25. **Liu, Q., C. Tackney, R. A. Bhat, A. M. Prince, and P. Zhang.** 1997. Regulated processing of hepatitis C virus core protein is linked to subcellular localization. J. Virol. 71:657–662.
26. **Lo, S. Y., M. J. Selby, and J. H. Ou.** 1996. Interaction between hepatitis C virus core protein and E1 envelope protein. J. Virol. 70:5177–5182.
27. **Marchuk, D., M. Drumm, A. Saulino, and F. S. Collins.** 1991. Construction of T-vectors, a rapid and general system for direct cloning of unmodified PCR products. Nucleic Acids Res. 19:1154.
28. **Martoglio, B., and B. Dobberstein.** 1998. Signal sequences: more than just greasy peptides. Trends Cell. Biol. 8:410–415.
29. **Marusawa, H., M. Hijikata, T. Chiba, and K. Shimotohno.** 1999. Hepatitis C virus core protein inhibits Fas- and tumor necrosis factor alpha-mediated apoptosis via NF-kappaB activation. J. Virol. 73:4713–4720.
30. **McLauchlan, J., M. K. Lemberg, G. Hope, and B. Martoglio.** 2002. Intramembrane proteolysis promotes trafficking of hepatitis C virus core protein to lipid droplets. EMBO J. 21:3980–3988.
31. **Moradpour, D., T. Wakita, K. Tokushige, R. I. Carlson, K. Krawczynski, and J. R. Wands.** 1996. Characterization of three novel monoclonal antibodies against hepatitis C virus core protein. J. Med. Virol. 48:234–241.
32. **Morishi, K., M. Koura, and Y. Matsuura.** 2002. Induction of Bad-mediated

apoptosis by Sindbis virus infection: involvement of pro-survival members of the Bcl-2 family. Virology 292:258–271.
33. **Morilishi, K., T. Okabayashi, K. Nakai, K. Moriya, K. Koike, S. Murata, T. Chiba, K. Tanaka, R. Suzuki, T. Suzuki, T. Miyamura, and Y. Matsuura.** 2003. Proteasome activator PA28γ-dependent nuclear retention and degradation of hepatitis C virus core protein. J. Virol. 77:10237–10249.
34. **Moriya, K., H. Fujie, Y. Shintani, H. Yotsuyanagi, T. Tsutsumi, K. Ishibashi, Y. Matsuura, S. Kimura, T. Miyamura, and K. Koike.** 1998. The core protein of hepatitis C virus induces hepatocellular carcinoma in transgenic mice. Nat. Med. 4:1065–1067.
35. **Moriya, K., H. Fujie, H. Yotsuyanagi, Y. Shintani, T. Tsutsumi, Y. Matsuura, T. Miyamura, S. Kimura, and K. Koike.** 1997. Subcellular localization of hepatitis C virus structural proteins in the liver of transgenic mice. Jpn. J. Med. Sci. Biol. 50:169–177.
36. **Moriya, K., H. Yotsuyanagi, Y. Shintani, H. Fujie, K. Ishibashi, Y. Matsuura, T. Miyamura, and K. Koike.** 1997. Hepatitis C virus core protein induces hepatic steatosis in transgenic mice. J. Gen. Virol. 78:1527–1531.
37. **Munro, S., and H. R. Pelham.** 1987. A C-terminal signal prevents secretion of luminal ER proteins. Cell 48:899–907.
38. **Paetzel, M., A. Karla, N. C. Strynadka, and R. E. Dalbey.** 2002. Signal peptidases. Chem. Rev. 102:4549–4580.
39. **Pelham, H. R.** 1996. The dynamic organisation of the secretory pathway. Cell Struct. Funct. 21:413–419.
40. **Ray, R. B., K. Meyer, R. Steele, A. Shrivastava, B. B. Aggarwal, and R. Ray.** 1998. Inhibition of tumor necrosis factor (TNF-alpha)-mediated apoptosis by hepatitis C virus core protein. J. Biol. Chem. 273:2256–2259.
41. **Ruggieri, A., T. Harada, Y. Matsuura, and T. Miyamura.** 1997. Sensitization to Fas-mediated apoptosis by hepatitis C virus core protein. Virology 229: 68–76.
42. **Saito, I., T. Miyamura, A. Ohbayashi, H. Harada, T. Katayama, S. Kikuchi, Y. Watanabe, S. Koi, M. Onji, Y. Ohta, Q. Choo, M. Houghton, and G. Kuo.** 1990. Hepatitis C virus infection is associated with the development of hepatocellular carcinoma. Proc. Natl. Acad. Sci. USA 87:6547–6549.
43. **Santolini, E., G. Migliaccio, and N. La Monica.** 1994. Biosynthesis and biochemical properties of the hepatitis C virus core protein. J. Virol. 68: 3631–3641.
44. **Selby, M. J., Q. L. Choo, K. Berger, G. Kuo, E. Glazer, M. Eckart, C. Lee, D. Chien, C. Kuo, and M. Houghton.** 1993. Expression, identification and subcellular localization of the proteins encoded by the hepatitis C viral genome. J. Gen. Virol. 74:1103–1113.
45. **Shoji, I., T. Suzuki, M. Sato, H. Aizaki, T. Chiba, Y. Matsuura, and T. Miyamura.** 1999. Internal processing of hepatitis C virus NS3 protein. Virology 254:315–323.
46. **Shrivastava, A., S. K. Manna, R. Ray, and B. B. Aggarwal.** 1998. Ectopic expression of hepatitis C virus core protein differentially regulates nuclear transcription factors. J. Virol. 72:9722–9728.
47. **Suzuki, R., Y. Matsuura, T. Suzuki, A. Ando, J. Chiba, S. Harada, I. Saito, and T. Miyamura.** 1995. Nuclear localization of the truncated hepatitis C virus core protein with its hydrophobic C terminus deleted. J. Gen. Virol. 76:53–61.
48. **Takamizawa, A., C. Mori, I. Fuke, S. Manabe, S. Murakami, J. Fujita, E. Onishi, T. Andoh, I. Yoshida, and H. Okayama.** 1991. Structure and organization of the hepatitis C virus genome isolated from human carriers. J. Virol. 65:1105–1113.
49. **Vallejo, A. N., R. J. Pogulis, and L. R. Pease.** 1995. Mutagenesis and synthesis of novel recombinant genes using PCR, p. 603–612. *In* C. W. Dieffenbach and G. S. Dveksler (ed.), PCR primer: a laboratory manual. Cold Spring Harbor Laboratory Press, Cold Spring Harbor, N.Y.
50. **Weihofen, A., K. Binns, M. K. Lemberg, K. Ashman, and B. Martoglio.** 2002. Identification of signal peptide peptidase, a presenilin-type aspartic protease. Science 296:2215–2218.
51. **Weihofen, A., M. K. Lemberg, H. L. Ploegh, M. Bogyo, and B. Martoglio.** 2000. Release of signal peptide fragments into the cytosol requires cleavage in the transmembrane region by a protease activity that is specifically blocked by a novel cysteine protease inhibitor. J. Biol. Chem. 275:30951–30956.
52. **Weihofen, A., and B. Martoglio.** 2003. Intramembrane-cleaving proteases: controlled liberation of proteins and bioactive peptides. Trends Cell Biol. 13:71–78.
53. **Yasui, K., T. Wakita, K. Tsukiyama-Kohara, S. I. Funahashi, M. Ichikawa, T. Kajita, D. Moradpour, J. R. Wands, and M. Kohara.** 1998. The native form and maturation process of hepatitis C virus core protein. J. Virol. 72:6048–6055.
54. **You, L. R., C. M. Chen, and Y. H. Lee.** 1999. Hepatitis C virus core protein enhances NF-κB signal pathway triggering by lymphotoxin-beta receptor ligand and tumor necrosis factor alpha. J. Virol. 73:1672–1681.
55. **Zhu, N., A. Khoshnan, R. Schneider, M. Matsumoto, G. Dennert, C. Ware, and M. M. Lai.** 1998. Hepatitis C virus core protein binds to the cytoplasmic domain of tumor necrosis factor (TNF) receptor 1 and enhances TNF-induced apoptosis. J. Virol. 72:3691–3697.

JOURNAL OF VIROLOGY, Oct. 2004, p. 10820–10824 Vol. 78, No. 19
0022-538X/04/$08.00+0 DOI: 10.1128/JVI.78.19.10820–10824.2004

Identification of Basal Promoter and Enhancer Elements in an Untranslated Region of the TT Virus Genome

Tetsuro Suzuki,[1]* Ryosuke Suzuki,[1] Jin Li,[1] Minako Hijikata,[2] Mami Matsuda,[1] Tiang-Cheng Li,[1] Yoshiharu Matsuura,[3] Shunji Mishiro,[4] and Tatsuo Miyamura[1]

Department of Virology II, National Institute of Infectious Diseases,[1] and Department of Respiratory Diseases, Research Institute, International Medical Center of Japan,[2] Shinjuku-ku, and Department of Medical Sciences, Toshiba General Hospital, Shinagawa-ku,[4] Tokyo, and Research Center for Emerging Infectious Diseases, Research Institute for Microbial Diseases, Osaka University, Suita-shi, Osaka,[3] Japan

Received 2 April 2004/Accepted 19 May 2004

The regulation of TT virus (TTV) gene expression was characterized. Transient-transfection assays using reporter constructs revealed that a 113-nucleotide (nt) sequence within the untranslated region, proximal to the transcription initiation site and containing a TATA box motif, has a basal promoter activity. This sequence is well conserved among different TTV genotypes. Upstream stimulating factor bound to a consensus binding motif within this region and positively regulates TTV transcription. Furthermore, a 488-nt region upstream of the basal promoter exhibited enhancer activity, presumably in a cell type-specific manner. This study illustrates some of the mechanisms involved in the transcriptional regulation of TTV.

TT virus (TTV), which was discovered in a patient with acute hepatitis, is an unenveloped, single-stranded, circular DNA virus, with a genome of approximately 3.8 kb (6). TTV is thought to be a new member of the *Circoviridae* family of viruses, and it was recently proposed that the virus be named Torque Teno virus (6). The TTV genome includes an untranslated region (UTR) of approximately 1.2 kb and a coding region of approximately 2.6 kb, including two major open reading frames which are sandwiched by the TATA box and polyadenylation signal motifs (11, 13, 15). Analyses of TTV transcripts have revealed three spliced mRNA species of 3.0, 1.2, and 1.0 kb with common 5′ and 3′ termini (9, 14). However, the molecular mechanisms controlling TTV transcription are still unknown. In this study, the basal promoter and enhancer of a TTV isolate, SANBAN of genogroup 3 (5, 18), were identified and functionally characterized.

First, we determined the transcription initiation sites of the TTV genome by 5′ rapid amplification of cDNA end (5′-RACE) analysis (Marathon cDNA amplification kit; Clontech) using poly(A)-rich RNA from a human hepatocellular carcinoma cell line, HepG2, transfected with a cloned TTV genome. The 5′-RACE PCR products were cloned and sequenced. We observed two potential transcription initiation sites, which map at nucleotides (nt) 121 and 110 (numbered according to the sequence deposited in DDBJ/GenBank/EMBL databases under accession number AB025946). Although transcription may be initiated at both sites, the upper site was designated position +1 in this study.

The UTR of the TTV genome contains a TATA box element between positions −40 and −35, as well as a number of putative transcription factor-binding motifs (Fig. 1A). Despite considerable genetic diversity throughout the whole genome, the UTR sequence was relatively conserved among the different TTV genotypes, presumably reflecting its functional constraints (15, 16). Thus, we analyzed transcriptional regulation of the UTR sequence.

To characterize TTV promoter activity, a firefly luciferase reporter plasmid, p(−890/+115), was constructed by subcloning the TTV sequence from positions −890 to +115, which was amplified by PCR using appropriate primers with restriction sites at the 5′ ends, into the promoterless pGL3-Basic (Promega). Eleven different cell lines were transfected with p(−890/+115), along with a *Renilla* luciferase expression vector, pRL-TK, as an internal standard for determining transfection efficiency. Luciferase activities in cell lysates prepared after 16 h of transfection were determined (2). It is of interest that the 1.0-kb fragment demonstrated a pronounced promoter activity in all the hepatocellular carcinoma cell lines tested. Human (Huh7, HepG2, and FLC4 [1, 2]) and mouse (Hepa1-clc7) hepatocellular carcinoma cells were tested (Fig. 1B). This fragment demonstrated the greatest activity in Huh7 cells (~10-fold greater than in other cells). We observed substantial promoter activity in GL37 (African green monkey kidney) and CHO (Chinese hamster ovary) cells, whereas limited activity was observed in Caco2 (human colon carcinoma), MOLT4 (human T-cell leukemia), CV1 (African green monkey kidney fibroblast), 3T3 Swiss (mouse fibroblast), and CMT93 (mouse rectal carcinoma) cells. These results indicate that the UTR of the TTV genome functions as a promoter in a cell type-specific manner.

To assess basal, proximal promoter activity in the UTR, a series of 5′ deletions fused to the luciferase gene were constructed and transfected into Huh7 and HepG2 cells (Fig. 2). A deletion extending to nt −601 [p(−601/+115)] enhanced promoter activity in both cell lines (by ~1.5-fold), while deletion of another 274 nt [p(−327/+115)] decreased promoter activity by more than 80%, suggesting that there is a negative regula-

* Corresponding author. Mailing address: Department of Virology II, National Institute of Infectious Diseases, 1-23-1 Toyama, Shinjuku-ku, Tokyo 162-8640, Japan. Phone: (81) 3-5285-1111. Fax: (81) 3-5285-1161. E-mail: tesuzuki@nih.go.jp.

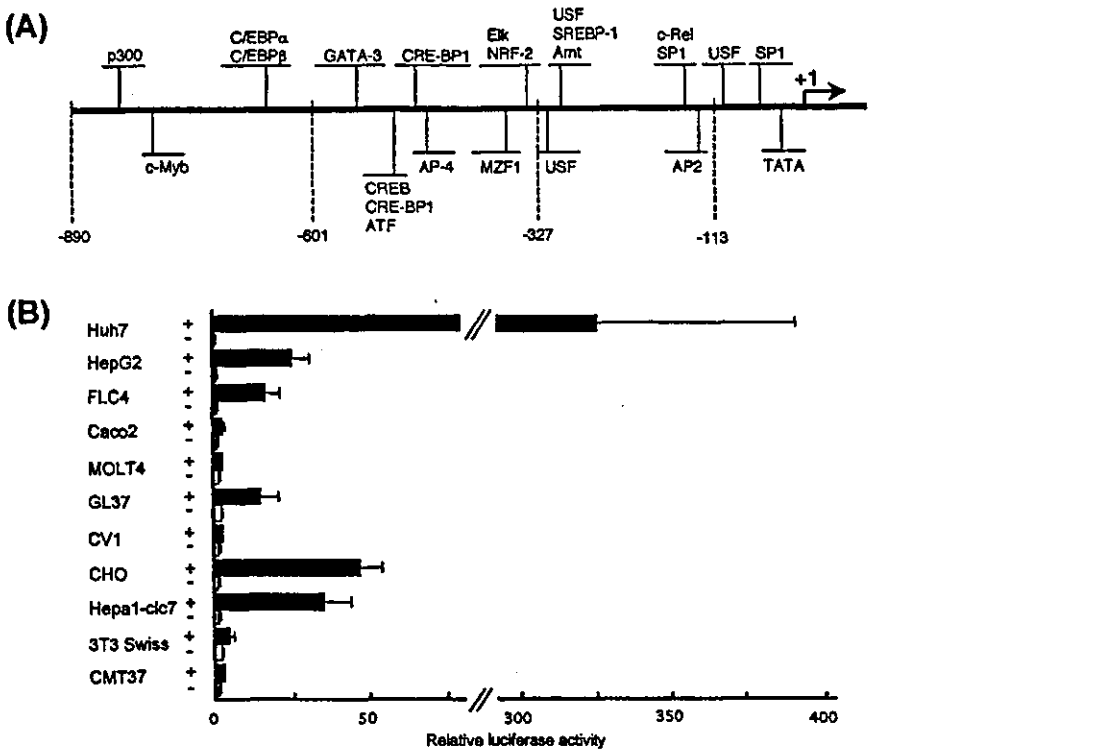

FIG. 1. Functional analysis of the TTV promoter in the viral UTR. (A) Schematic representation of the 1.0-kb UTR sequence. The TATA box element and putative transcription factor-binding sites are shown. Transcription factor-binding sites were identified using the TRASFAC database and a search program (http://motif.genome.ad.jp/). The transcription initiation site (+1) is indicated and corresponds to nt 121 (AB025946). The numbers at the bottom of vertical dotted lines indicate the start points of the full-length promoter construct and deletion mutants of the promoter constructs used in Fig. 1B and 2. (B) Cell type specificity of the TTV promoter activities. Cells were transfected with p(−890/+115) (+) or promoter-less pGL3-Basic (−) together with pRL-TK (*Renilla* luciferase). Cell extracts were prepared 16 h after transfection, and luciferase activities in the extracts were determined using a dual-luciferase reporter assay system (Promega) with the Lumat LB9501 luminometer (Berthold). All values were normalized to *Renilla* luciferase activities and are shown as means ± standard deviations (error bars) of three independent samples.

tory element between nt −890 and −601. A deletion extending to nt −113 [p(−113/+115)] resulted in a slight to moderate reduction in activity, but promoter activity still remained greater than that observed with p(+15/+113), in which the TATA box and the transcription start sites were deleted. These findings suggest that the 113 nt immediately upstream of the transcription initiation site contains a basal promoter region critical for TTV gene expression.

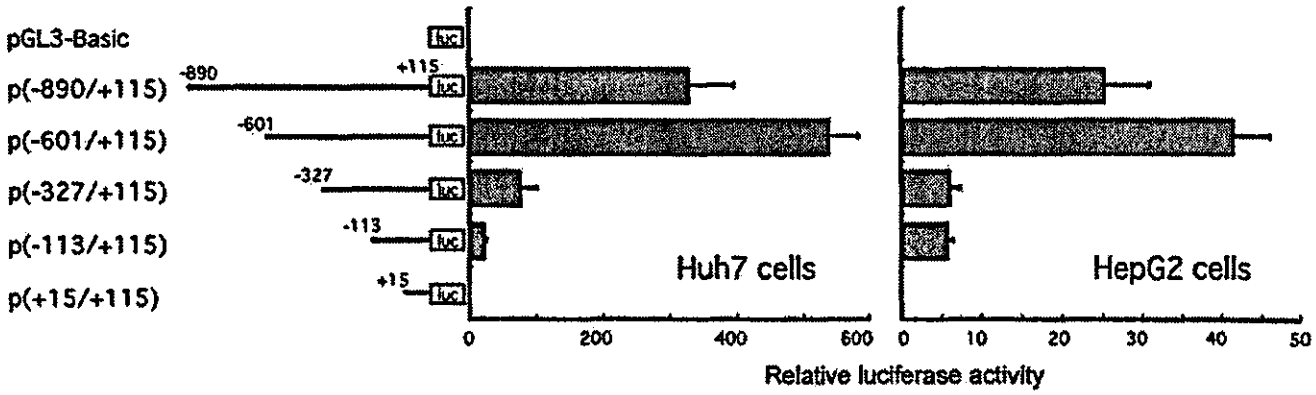

FIG. 2. Deletion analysis of the TTV promoter in Huh7 and HepG2 cells. The structures of the luciferase reporter constructs containing various lengths of the TTV UTR sequence are shown to the left. A series of DNA fragments with 5′ deletions of the TTV promoter were amplified by PCR using the full-length TTV DNA of SANBAN isolate as a template with the same reverse primer and various forward primers. The fragments were cloned into pGL3-Basic at XhoI and HindIII sites. The indicated constructs were transfected into Huh7 cells or HepG2 cells. Relative luciferase activity in each transfectant was determined as described in the legend to Fig. 1B. Results are shown as means ± standard deviations (error bars) of three independent samples.

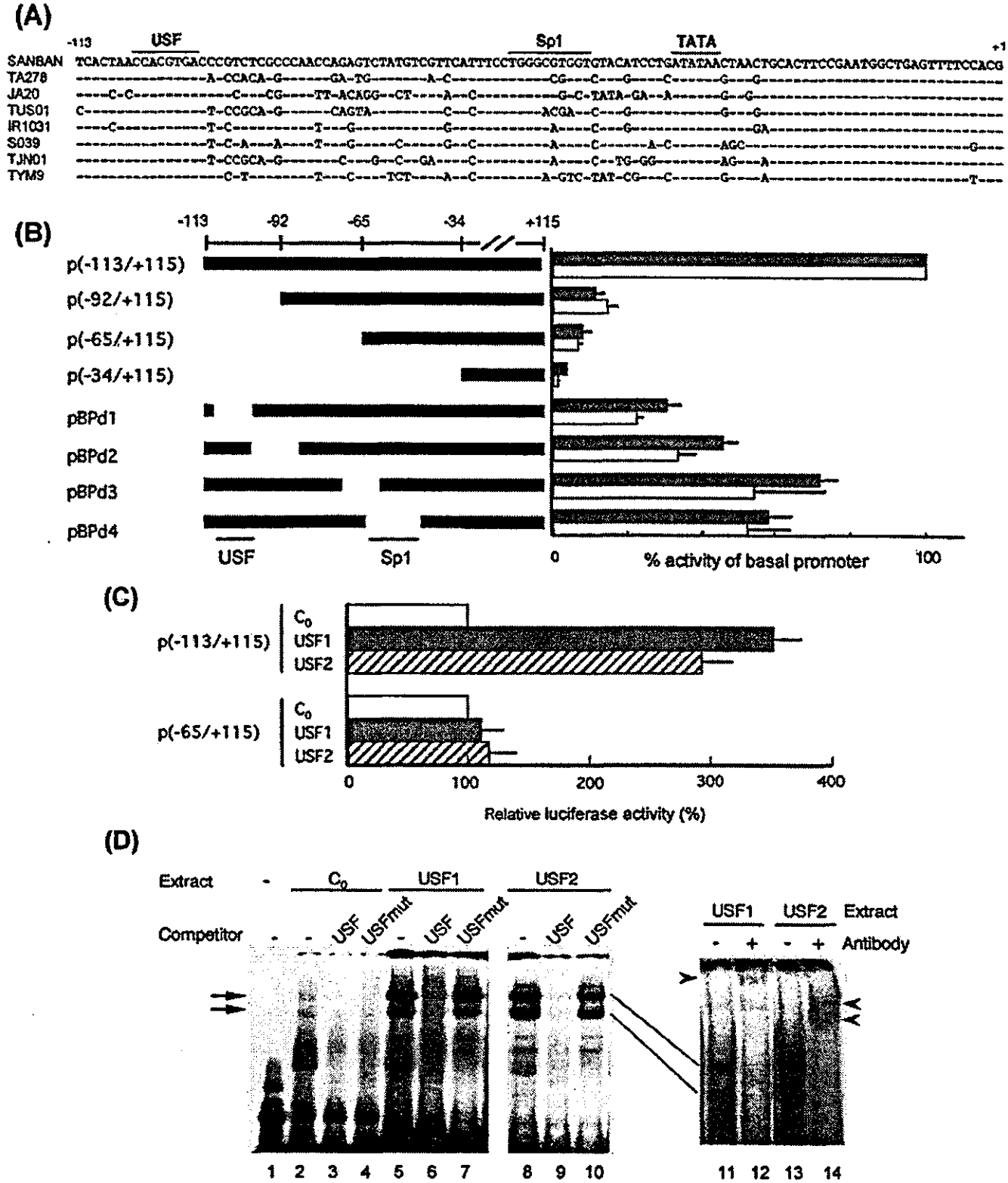

FIG. 3. Basal promoter activity of TTV regulated by USF. (A) Alignment of the putative basal promoter regions from TTV isolates SANBAN (DDBJ/GenBank/EMBL accession number AB025946), TA278 (AB017911), JA20 (AF122914), TUS01 (AB017613), IR1031 (AB038619), S039 (AB038620), TJN01 (AB028668), and TYM9 (AB050448). The transcription initiation site is numbered +1. The TATA box and positions of putative binding sites for USF and SP1 are indicated. Nucleotides that are identical to those in the SANBAN isolate (−) are indicated. (B) Effect of deleting DNA from the basal promoter region on the TTV basal promoter activity. A series of DNA fragments with 5′ or internal deletions of the basal promoter region were amplified by PCR and cloned into pGL3-Basic at XhoI and HindIII sites. The indicated constructs were transfected into Huh7 cells (gray bars) or HepG2 cells (white bars). Relative luciferase activity in each transfectant was determined as described in the legend

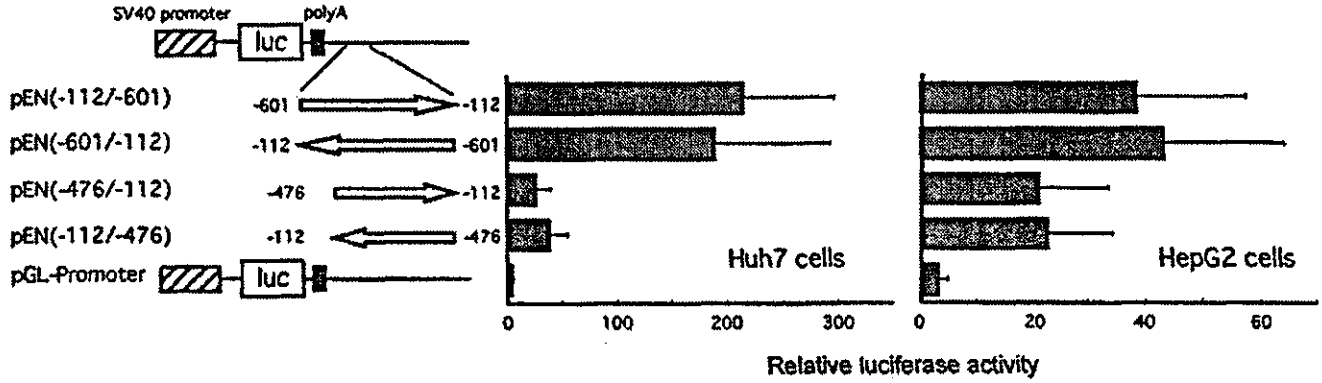

FIG. 4. Enhancer activity of the 488-nt fragment (−601/−114) of the TTV UTR. The 488-nt (−614/−114) and 363-nt (−476/−114) fragments were PCR amplified using primers with 5′ overhangs containing BglII (sense) and BamHI (antisense) sites. The fragments were then cloned into pGL3-Promoter at the BamHI site. The indicated constructs (left panel) were transfected into Huh7 cells or HepG2 cells. Relative luciferase activity in each transfectant was determined as described in the legend to Fig. 1B. Results are shown as means ± standard deviations (error bars) of three independent samples. SV40, simian virus 40.

Computer-assisted analysis of this basal promoter region identified potential binding sites recognized by upstream stimulating factor (USF) and Sp1, which are conserved among TTV genotypes (Fig. 3A). To determine whether these sequences contribute to TTV promoter activity, 5′ or internal deletion mutations were introduced into p(−113/+115), which was then examined for dual luciferase activity. Deletions, those found in p(−92/+115) and pBPd1, reduced promoter activity by 70 to 85%, suggesting that the USF-binding sequence is crucial for TTV promoter activity (Fig. 3B). Deletion of a Sp1-binding sequence (pBPd4) also conferred a decrease in promoter activity, although their effects were relatively moderate, suggesting that the Sp1-binding motif and/or its encompassing sequence may play a role in regulating TTV promoter activity by maintaining the structural integrity of the transcriptional machinery.

In genes where USF regulates transcription, cotransfection of USF expression vectors with reporter genes stimulates reporter activities. To further investigate the effect of USF on TTV promoter activity, we cotransfected USF1 or USF2 expression vectors (pCMV-USF1 and pCMV-USF2) (7) with p(−113/+115) into HepG2 cells. The cotransfection significantly increased promoter activity (by threefold), suggesting that USF proteins regulate TTV transcription (Fig. 3C).

USF is a family of basic-helix-loop-helix-leucine zipper transcription factors, initially identified by their ability to bind to the 5′-CACGTG-3′ sequence within the adenovirus major late promoter (3, 4, 10). USF1 and USF2 have been subsequently shown to bind to the promoters of various cellular and viral genes. To determine whether the TTV basal promoter was capable of USF binding, gel mobility shift assays were performed on an end-labeled oligonucleotide (nt −113 to −84) containing the putative USF-binding motif (Fig. 3D). DNA-protein-binding complexes were observed in nuclear extracts from cells transfected with pCMV-USF1 (Fig. 3D, lane 5), pCMV-USF2 (lane 8), and the empty vector (lane 2). An excess of unlabeled homologous probe competed with the protein binding (lanes 3, 6, and 10), whereas a mutated USF sequence failed to compete (lanes 4, 7, and 10). The addition of anti-USF antibodies to the binding reaction mixture supershifted the DNA-protein complexes (lanes 12 and 14). The combined data demonstrate that USF binds to its binding motif within the TTV basal promoter to up-regulate viral transcription.

On the basis of the results of the luciferase assays using 5′ deletions of the TTV UTR (Fig. 2), the positive regulatory element appears to be located immediately upstream of the basal promoter. To ascertain whether the 488-bp fragment between nt −601 and −113 functions as the enhancer region, this fragment or a 5′ deletion of this fragment was placed downstream of the polyadenylation signal in pGL3-Promoter (Promega), driven by the simian virus 40 promoter, in either

to Fig. 1B. Results are shown as a percentage of the activity in cells transfected with p(−113/+115); values are shown as means ± standard deviations (error bars) (n = 3 per group). (C) Effects of USF overexpression on basal promoter activity. HepG2 cells were cotransfected with each reporter construct with pCMV-USF1 (USF1), pCMV-USF2 (USF2), or empty pC_0 vector (C_0). Luciferase activity was determined 48 h after transfection. For each reporter construct, relative luciferase activity is presented as a percentage of the activity in pC_0-transfected cells. (D) Binding of USF proteins to the region from nt −113 to −84 in the TTV basal promoter. The electrophoretic mobility shift assays were performed as described previously (19). A double-stranded oligonucleotide corresponding to the TTV sequence from nt −113 to −84 was used as a probe. Nuclear extracts from the cells transiently transfected with pCMV-USF1 (USF1; lanes 5, 6, 7, 11, and 12), pCMV-USF2 (USF2; lanes 8, 9, 10, 13, and 14), or pC_0 (C_0; lanes 2 to 4) or no extract (lane 1) were mixed with ^{32}P-labeled probe for the binding reaction mixtures. Competitors, unlabeled probe (USF), and a mutant with the USF-binding motif (USFmut) were added at a 25-fold molar excess. The sense sequence (5′-TCACTAAC CAATTGACCCGTCTCGCCCAAC [the mutated nucleotides are underlined]) and complementary sequence of the mutant with the USF-binding motif were added. A supershift experiment was also performed by incubating antibody against USF1 (lane 12) or USF2 (lane 14) (+) with the nuclear extracts before the probe was added. The positions of specific binding complexes (arrows) and supershifted complexes (arrowheads) are indicated.

the sense or antisense orientation. Luciferase activity of constructs containing the 488-bp fragment [pEN(−601/−114) and pEN(−114/−601)] led to 50- and 10-fold stimulation in Huh7 and HepG2 cells, respectively. The 5′ deletion extending to nt −476 [pEN(−476/−114) and pEN(−114/−476)] reduced enhancer activity (Fig. 4). No enhancement was observed by transfection of MOLT4 cells with pEN(−601/−114) and pEN(−114/−601) (data not shown). These results demonstrate that the 488-bp region upstream of the basal promoter contains an enhancer element, suggesting cell-specific transcription of the TTV genome. It is noteworthy that the enhancer element is conserved among TTV genotypes. For example, 72% homology has been observed between clones SANBAN and TA278, and the database search has revealed at least 20 potential transcription factor-binding sites within this element, including CREB and CRB, which are activated upon cyclic AMP signaling-dependent phosphorylation (12, 17).

While the manuscript was being prepared, Kamada et al. reported the promoter and enhancer activities in the UTR of TTV, clone VT416 whose genome is 98% similar to that of TA278, and its cell tropism (8). However, they did not identify transcription factors that bind to the region and regulate TTV transcription. In summary, the findings reported by Kamada et al. and the findings of our present study emphasize the important role of the UTR as a basal promoter and enhancer within the UTR. Other areas of interest for further study include the identification of additional factors involved in tissue-specific TTV transcription and determining the significance of polymorphism of the regulatory elements.

We are grateful to M. Sawadogo (University of Texas M. D. Anderson Cancer Center, Houston, Tex.) for providing pCMV-USF1, pCMV-USF2, and pC_0. We thank M. Yahata and S. Yoshizaki for technical assistance and T. Mizoguchi for preparation of the manuscript.

This work was supported in part by grants-in-aid from the Ministry of Health, Labor and Welfare of Japan.

REFERENCES

1. **Aizaki, H., S. Nagamori, M. Matsuda, H. Kawakami, O. Hashimoto, H. Ishiko, M. Kawada, T. Matsuura, S. Hasumura, Y. Matsuura, T. Suzuki, and T. Miyamura.** 2003. Production and release of infectious hepatitis C virus from human liver cell cultures in the three-dimensional radial-flow bioreactor. Virology 314:16–25.
2. **Aoki, Y., H. Aizaki, T. Shimoike, H. Tani, K. Ishii, I. Saito, Y. Matsuura, and T. Miyamura.** 1998. A human liver cell line exhibits efficient translation of HCV RNAs produced by a recombinant adenovirus expressing T7 RNA polymerase. Virology 250:140–150.
3. **Atchley, W. R., and W. M. Fitch.** 1997. A natural classification of the basic helix-loop-helix class of transcription factors. Proc. Natl. Acad. Sci. USA 94:5172–5176.
4. **Gregor, P. D., M. Sawadogo, and R. G. Roeder.** 1990. The adenovirus major late transcription factor USF is a member of the helix-loop-helix group of regulatory proteins and binds to DNA as a dimer. Genes Dev. 4:1730–1740.
5. **Hijikata, M., K. Takahashi, and S. Mishiro.** 1999. Complete circular DNA genome of a TT virus variant (isolate name SANBAN) and 44 partial ORF2 sequences implicating a great degree of diversity beyond genotypes. Virology 260:17–22.
6. **Hino, S.** 2002. TTV, a new human virus with single stranded circular DNA genome. Rev. Med. Virol. 12:151–158.
7. **Ismail, P. M., T. Lu, and M. Sawadogo.** 1999. Loss of USF transcriptional activity in breast cancer cell lines. Oncogene 18:5582–5591.
8. **Kamada, K., T. Kamahora, P. Kobat, and S. Hino.** 2003. Transcriptional regulation of TT virus: promoter and enhancer regions in the 1.2-kb noncoding region. Virology 321:341–348.
9. **Kamahora, T., S. Hino, and H. Miyata.** 2000. Three spliced mRNAs of TT virus transcribed from a plasmid containing the entire genome in COS1 cells. J. Virol. 74:9980–9986.
10. **Lin, Q., X. Luo, and M. Sawadogo.** 1994. Archaic structure of the gene encoding transcription factor USF. J. Biol. Chem. 269:23894–23903.
11. **Miyata, H., H. Tsunoda, A. Kazi, A. Yamada, M. A. Khan, J. Murakami, T. Kamahora, K. Shiraki, and S. Hino.** 1999. Identification of a novel GC-rich 113-nucleotide region to complete the circular, single-stranded DNA genome of TT virus, the first human circovirus. J. Virol. 73:3582–3586.
12. **Montminy, M.** 1997. Transcriptional regulation by cyclic AMP. Annu. Rev. Biochem. 66:807–822.
13. **Mushahwar, I. K., J. C. Erker, A. S. Muerhoff, T. P. Leary, J. N. Simons, L. G. Birkenmeyer, M. L. Chalmers, T. J. Pilot-Matias, and S. M. Dexai.** 1999. Molecular and biophysical characterization of TT virus: evidence for a new virus family infecting humans. Proc. Natl. Acad. Sci. USA 96:3177–3182.
14. **Okamoto, H., T. Nishizawa, A. Tawara, M. Takahashi, J. Kishimoto, T. Sai, and Y. Sugai.** 2000. TT virus mRNAs detected in the bone marrow cells from an infected individual. Biochem. Biophys. Res. Commun. 279:700–707.
15. **Okamoto, H., T. Nishizawa, and M. Ukita.** 1999. A novel unenveloped DNA virus (TT virus) associated with acute and chronic non-A to G hepatitis. Intervirology 42:196–204.
16. **Prescott, L. E., D. M. MacDonald, F. Davidson, J. Mokili, D. I. Pritchard, D. E. Arnot, E. M. Riley, B. M. Greenwood, S. Hamid, A. A. Saeed, M. O. McClure, D. B. Smith, and P. Simmonds.** 1999. Sequence diversity of TT virus in geographically dispersed human populations. J. Gen. Virol. 80:1751–1758.
17. **Sassone-Corsi, P.** 1998. Coupling gene expression to cAMP signalling: role of CREB and CREM. Int. J. Biochem. Cell. Biol. 30:27–38.
18. **Takahashi, K., M. Hijikata, E. I. Samokhvalov, and S. Mishiro.** 2000. Full or near full-length nucleotide sequences of TT virus variants (types SANBAN and YONBAN) and the TT virus-like mini virus. Intervirology 43:119–123.
19. **Tsutsumi, T., T. Suzuki, T. Shimoike, R. Suzuki, K. Moriya, Y. Shintani, H. Fujie, Y. Matsuura, K. Koike, and T. Miyamura.** 2002. Interaction of hepatitis C virus core protein with retinoid X receptor alpha modulates its transcriptional activity. Hepatology 35:937–946.

Available online at www.sciencedirect.com

SCIENCE DIRECT

Virology 324 (2004) 74–83

VIROLOGY

www.elsevier.com/locate/yviro

Pseudotype hepatitis C virus enters immature myeloid dendritic cells through the interaction with lectin

Aki Kaimori,[a] Tatsuya Kanto,[a,b] Chang Kwang Limn,[c] Yasumasa Komoda,[c] Chika Oki,[a] Michiyo Inoue,[a,b] Hideki Miyatake,[a] Ichiyo Itose,[a] Mitsuru Sakakibara,[a] Takayuki Yakushijin,[a] Tetsuo Takehara,[a] Yoshiharu Matsuura,[c] and Norio Hayashi[a,*]

[a] *Department of Molecular Therapeutics, Osaka University Graduate School of Medicine, Suita, Osaka 565-0871, Japan*
[b] *Department of Dendritic Cell Biology and Clinical Application, Osaka University Graduate School of Medicine, Suita, Osaka 565-0871, Japan*
[c] *Research Center for Emerging Infectious Diseases, Research Institute for Microbial Diseases, Osaka University, Suita, Osaka 565-0871, Japan*

Received 14 October 2003; returned to author for revision 12 November 2003; accepted 24 March 2004

Abstract

Dendritic cells (DC) are the most potent antigen-presenting cells that regulate immune responses. One of the mechanisms for hepatitis C virus (HCV) persistence is the ability of HCV to suppress DC function. Direct HCV infection to blood DC has been implicated for DC dysfunction. To clarify the susceptibility of each DC subset to HCV, we used pseudotype vesicular stomatitis virus (VSV) coated with chimeric HCV envelope glycoproteins (E1 and E2). We demonstrate that pseudotype VSV enters myeloid DC (MDC) but not plasmacytoid DC (PDC). The highest efficiency of pseudotype VSV entry to MDC was observed when MDC were cultured with GM-CSF. Such efficiency decreased when MDC are matured with the treatment of IL-4, CpG oligodeoxynucleotide, or CD40 ligand. Mannan inhibited pseudotype VSV entry to MDC, but Ca^{2+} chelators failed to do so. These results show that pseudotype VSV possessing HCV-E1 and E2 enters immature MDC through the interaction with lectins in a Ca^{2+}-independent manner.

Keywords: Hepatitis C virus; Envelope proteins; Pseudotype virus; Dendritic cells; Lectin

Introduction

Hepatitis C virus (HCV), a single-stranded plus-sense RNA virus belonging to the fraviviridae family (Miller and Purcell, 1990), causes persistent infection in more than 70% of infected patients. The most important feature of HCV persistence is the potential for liver disease progression from mild hepatitis to liver cirrhosis and hepatocellular carcinoma (HCC) (Alter et al., 1989). Chronic HCV infection is a serious health problem because the total number of HCV-positive HCC patients is growing worldwide. One of the mechanisms for HCV persistence is the ability of HCV to escape from the host cellular immune response (Farci et al., 1992; Weiner et al., 1995). Cumulative studies show that functional impairment of immunocompetent cells is found in patients with chronic HCV infection (Corado et al., 1997; Wedemeyer et al., 2002), suggesting that HCV has various arms for suppressing the immune response.

Dendritic cells (DC) are the most potent antigen-presenting cells (APC) that regulate various immune responses (Banchereau and Steinman, 1998; Hart, 1997). Blood DC mainly consist of two subsets, that is, myeloid and plasmacytoid DC (Liu, 2001). Myeloid DC (MDC) are characterized by their potent immunostimulatory properties for both primary and secondary T-cell responses against virus. Plasmacytoid DC (PDC), previously known as interferon (IFN)-producing cells, produce a large amount of type I IFN upon virus infection (Liu, 2001). However, some viruses such as

* Corresponding author. Department of Molecular Therapeutics, Osaka University Graduate School of Medicine, 2-2 Yamada-oka, Suita, Osaka 565-0871, Japan. Fax: +81-6-6879-3449.
E-mail address: hayashin@moltx.med.osaka-u.ac.jp (N. Hayashi).

0042-6822/$ - see front matter © 2004 Elsevier Inc. All rights reserved.
doi:10.1016/j.virol.2004.03.038

measles virus or HIV have been shown to infect monocyte-derived DC (MoDC) or PDC and subsequently inhibit their immunostimulatory functions (Grosjean et al., 1997; Patterson et al., 2001; Schnorr et al., 1997). Previous studies including our own have shown that MoDC from patients with chronic HCV infection are functionally impaired (Bain et al., 2001; Kanto et al., 1999). In addition, our recent investigation revealed that the function of both types of blood DC is suppressed as well in HCV-infected patients (Kanto T. et al., unpublished data). These results led us to hypothesize that HCV infection to DC is one of the mechanism for DC dysfunction in chronic hepatitis C patients.

The existence of the HCV genome in blood cells including DC has been shown in several studies by means of reverse transcription (RT)-PCR (Bain et al., 2001; Lerat et al., 1996, 1998; Navas et al., 2002). The detection of the positive strand of HCV-RNA does not enable to define whether HCV enters cells or only adheres to their surface. Alternatively, the negative strand of HCV-RNA has been used as a surrogate marker of HCV replication (Navas et al., 2002). Recently, Matsuura et al. (2001) established the pseudotype vesicular stomatitis virus (VSV) having chimeric HCV E1 and E2 protein as an envelope (VSV-E1E2). Because it has a green fluorescent protein (GFP) reporter gene in its genome, the infected cells can be viewed under fluorescence. Using this system, we tried to clarify the susceptibility of each DC to HCV. Consequently, we demonstrate that MDC is susceptible to VSV-E1E2 but PDC is not. Furthermore, we showed that the lectin-containing molecules on MDC are critically involved in VSV-E1E2 entry. Our study provides useful information for the exploration of target molecules that efficiently block HCV entry to DC.

Results

Immature MDC are susceptible to VSV-E1E2

We inoculated pseudotype VSV on various cells separated from PBMC or cord blood. Because no positive fluorescence was obtained from CD4 T cells, CD8 T cells, B cells, NK cells, and fresh PDC inoculated with VSV ΔG-G which is complemented with the VSV G protein, the susceptibility of these cells to VSV-E1E2 could not be estimated. In contrast, VSV ΔG-G entered fresh MDC, monocytes, and $CD34^+$ hematopoietic precursor cells on the day of separation, whereas VSV-E1E2 and VSV ΔG did not. Thus, fresh MDC as well as DC precursors are not susceptible to VSV-E1E2 (Fig. 1).

To examine the influence of differentiation or maturation of DC on the susceptibility to the pseudotype VSV, MDC were cultured in the presence of GM-CSF with or without IL-4. Phenotypic analysis revealed that day 4 MDC cultured with GM-CSF and IL-4 had higher expression of CD1a and CD86 than those cultured with GM-CSF only (Fig. 2), showing the role of IL-4 in DC maturation. No significant difference was observed in the expression of CD11c, CD40, CD80, CD83, and HLA-DR between these MDC (Fig. 2). On day 4 of culture in the presence of IL-3, PDC showed higher expressions of CD40, CD80, CD83, and CD86 when compared to the day of separation (data not shown).

After the inoculation with VSV ΔG-G, positive signals were obtained from day 4 MDC and day 4 PDC, regardless of the difference of cytokines used (Figs. 3A and B). No significant signals were detected from day 4 MDC and day 4 PDC inoculated with VSV ΔG. With respect to VSV-E1E2, GFP^+ cells were observed in day 4 MDC but not in day 4 PDC (Figs. 3A and B). In

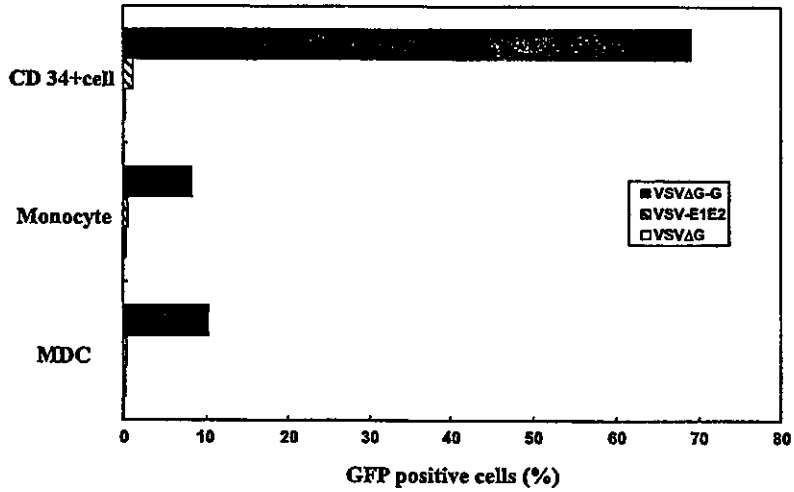

Fig. 1. Freshly isolated DC are not susceptible to VSV-E1E2. Freshly isolated $CD34^+$ hematopoietic precursor cells, monocytes, or MDC were inoculated with pseudotype VSVs and the percentages of GFP^+ cells were determined by flow cytometry. Representative results from three experiments are shown.

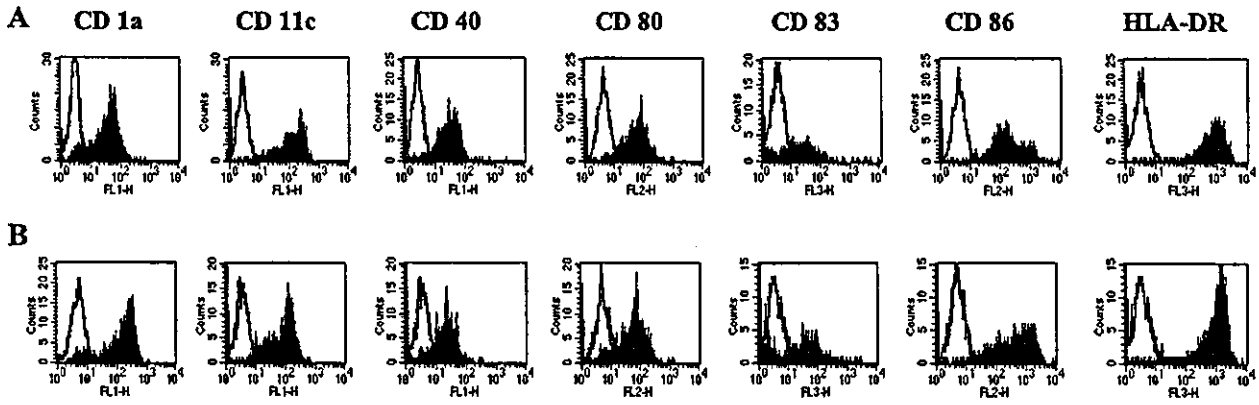

Fig. 2. Phenotypes of MDC cultured with GM-CSF or GM-CSF and IL-4. Flow cytometric analyses of surface molecules on day 4 MDC, obtained from healthy volunteers, cultured with GM-CSF (A) or with GM-CSF and IL-4 (B). Representative results from three subjects are shown. Open histograms represent the results with isotype Ab and filled ones represent those with relevant Abs. Fluorescence intensity is shown in the *x*-axis and the number of cells is shown in the *y*-axis.

comparison of the culture conditions for MDC, higher percentage of GFP^+ cells was observed in day 4 MDC cultured with only GM-CSF than those with GM-CSF and IL-4 (Fig. 3B).

To confirm the reliability of the pseudotype VSV system in the assessment of E1E2-mediated virus entry, we quantified HCV-RNA in day 4 cultured MDC or PDC after inoculation of a window-period serum from a hepatitis C patient. Among the cells examined, the highest HCV RNA titer was detected in day 4 MDC cultured with GM-CSF (Fig. 3C), which was compatible with the results obtained with the pseudotype VSV. In contrast with the results of VSV-E1E2 inoculation, low-level HCV RNA were detected by quantitative RT-PCR in PDC inoculated with authentic HCV (Fig. 3C). To further investigate whether HCV replicates in each DC subset after HCV inoculation, we performed strand-specific RT-PCR for the detection of negative-strand HCV-RNA as a surrogate marker of HCV replication. Positive strand of HCV-RNA was detected both in MDC cultured with GM-CSF and PDC with IL-3, whereas negative strand was detected in GM-CSF-MDC but not in IL-3-PDC (Fig. 3D). These results suggest that HCV replicates in GM-CSF-MDC but not in IL-3-PDC. Therefore, the data with the pseudotype VSV system correctly reflect the susceptibility of cells to authentic HCV.

Maturation stimuli protect MDC from VSV-E1E2

Based on the findings described above, we hypothesized that the more MDC mature, the less susceptible they are to VSV-E1E2. To find the substances protecting DC from HCV infection, we treated MDC with various maturation factors for the inoculation study. In MDC cultured with GM-CSF, the addition of IL-4, CpG oligodeoxynucleotide (ODN) 2006, or CD40 ligand (CD 40L) to the culture significantly reduced the percentage of GFP^+ cells with VSV-E1E2 without influencing their susceptibility to VSV ΔG-G (Fig. 4). On the other hand, IFN-α, polyI:C, TNF-α, and lipopolysaccharide (LPS) reduced the percentage of GFP^+ cells with both VSV-E1E2 and VSV ΔG-G (Fig. 4). Phenotypic analysis revealed that IL-4 up-regulated the expression of CD1a and CD86 on MDC cultured with GM-CSF (Fig. 2). CpG ODN or CD40L also up-regulated the expression of CD1a, CD83, and CD86 on MDC cultured with GM-CSF (data not shown). Therefore, immature DC lose their susceptibility to VSV-E1E2 as they develop to be more mature state.

Lectin on DC is involved in VSV-E1E2 entry to DC

The C-type lectins expressed on DC are reported to interact with various viruses as well as microbial agents (Geijtenbeek et al., 2000; Tailleux et al., 2003). These studies led us to consider the involvement of lectins in VSV-E1E2 entry to DC. Thus, we first used mannan to examine whether it inhibits VSV-E1E2 entry to MDC. The pretreatment of MDC with mannan reduced the percentage of GFP^+ cells with VSV-E1E2 in a dose-dependent manner without having any impact on VSV ΔG-G entry (Fig. 5A). Such an inhibitory effect of mannan was confirmed with MDC inoculated with authentic HCV (data not shown). A D-mannose-specific lectin, methyl α-D-mannopyranoside (Kaku et al., 1991), also inhibited VSV-E1E2 entry to MDC in a dose-dependent fashion at concentrations from 10 to 40 μg/ml (data not shown). In contrast, galactose had no effect on the infection with either VSV-E1E2 or VSV ΔG-G in MDC (Fig. 5A). Interestingly, EDTA did not reduce the infectivity of VSV-E1E2, whereas it completely abolished that of VSV ΔG-G (Fig. 5A). These data demonstrate that mannose-type carbohydrate is involved in the interaction of DC with VSV-E1E2 in a Ca^{2+}-independent manner. The treatment of MDC with antihuman DC-SIGN Ab,

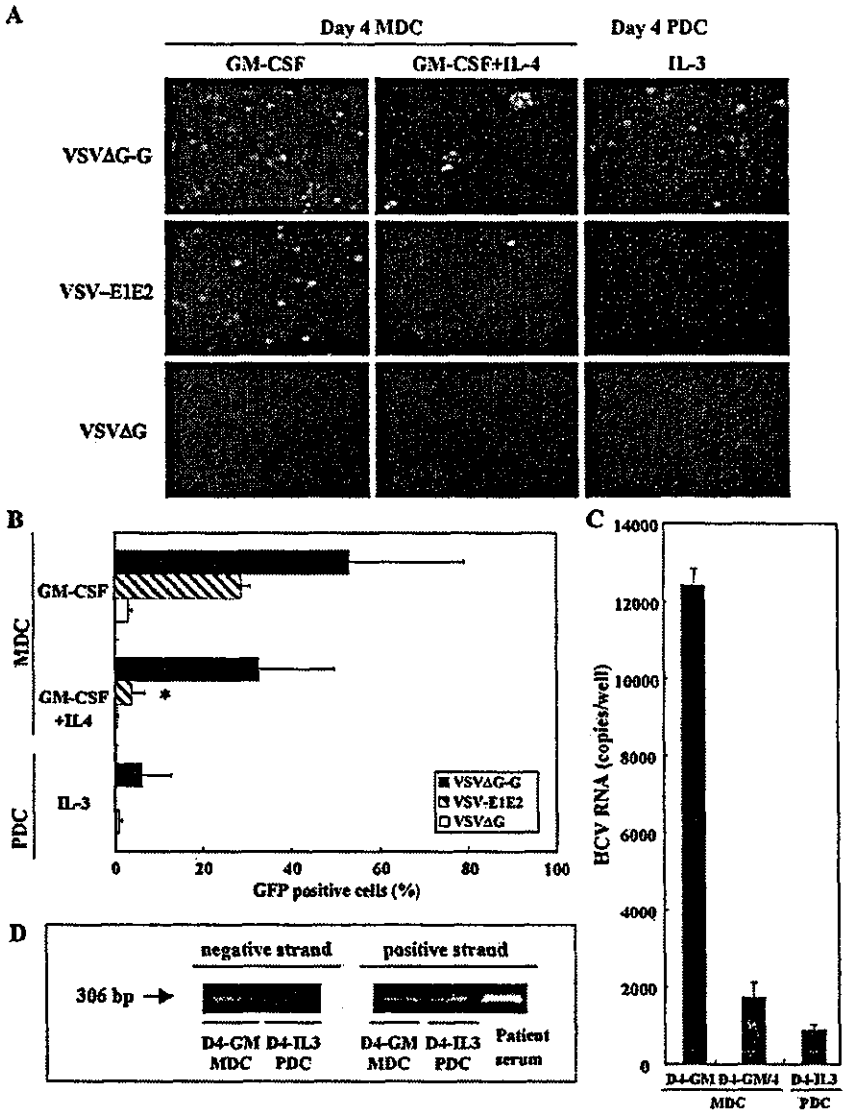

Fig. 3. Myeloid DC cultured with GM-CSF are susceptible to VSV-E1E2 or authentic HCV from patient serum. Day 4 MDC cultured with GM-CSF or with GM-CSF and IL-4 or day 4 PDC cultured with IL-3 were inoculated with VSV ΔG, VSV ΔG-G, or VSV-E1E2. They were viewed under fluorescence microscopy (A) and the percentages of GFP^+ cells were analyzed by flow cytometric analysis (B). The results of fluorescence microscopy are the representative ones from three subjects. The results of flow cytometric analysis are expressed as the mean + SD from three representative experiments. $^*P < 0.001$ vs. VSV-E1E2-inoculated day 4 MDC cultured with GM-CSF. (C) Quantitative analysis of HCV RNA in DC inoculated with HCV-positive patient serum was performed as described in Materials and method. D4-GM or D4-GM/4 represents MDC cultured with GM-CSF or GM-CSF and IL-4 for 4 days. D4-IL 3 represents PDC cultured with IL-3 for 4 days. The results are expressed as the mean + SD of triplicate wells from three representative experiments. (D) The detection of positive and negative strand of HCV-RNA in DC inoculated with HCV-positive patient serum. Strand-specific RT-PCR was performed with samples from MDC, PDC, and patient serum used as inoculum, as described in Materials and method. D4-GM and D4-IL 3 represent as the same as above.

which is able to block the binding of DC-SIGN to ICAM-3 (Wu et al., 2002), did not inhibit the entry of either VSV-E1E2 or VSV ΔG-G (Fig. 5B). To see whether the expression of DC-SIGN on MDC parallels their susceptibility to VSV-E1E2, we compared the expression of DC-SIGN between MDC cultured with GM-CSF and those with a combination of GM-CSF and IL-4. The expression of DC-SIGN was higher on MDC cultured with GM-CSF and IL-4 than on those with GM-CSF (Fig. 5C), which is contrary to their susceptibility to VSV-E1E2. These results show that DC-SIGN is less likely to be involved in the VSV-E1E2 entry to MDC. Human hepatoblastoma cell line, HepG2, is one of the most sensitive cells to pseudotype VSV (Matsuura et al., 2001). To compare the machinery of VSV-E1E2 entry between MDC and HepG2, we inoculated it to mannan-treated HepG2. In contrast to MDC, mannan did not inhibit the VSV-E1E2 entry to HepG2 (Fig. 5D), suggest-

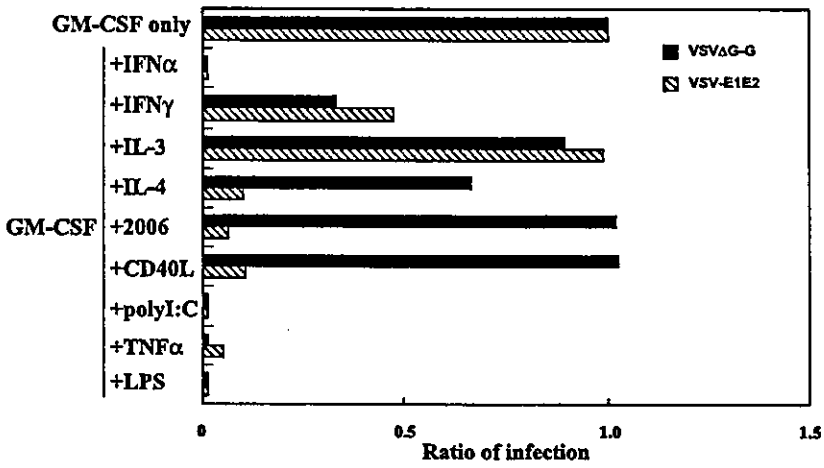

Fig. 4. IL-4, CpG ODN, or CD40L protects MDC from VSV-E1E2. Various immunomodulators were added to MDC cultured with GM-CSF, and the ratio of infection was determined between the cells treated with or without the reagents. IFN-α (100 U/ml), IFN-γ (100 U/ml), IL-3 (50 ng/ml), or IL-4 (10 ng/ml) was added on the day of MDC separation. CpG ODN 2006 (10 μM), CD40L (1 μg/ml), polyI:C (50 μg/ml), TNFα (20 ng/ml), or LPS (10 μg/ml) was added to MDC 24 hrs before the pseudovirus inoculation. Representative results are shown from three independent experiments.

ing that the molecules responsible for VSV-E1E2 entry differ between HepG2 and MDC. Furthermore, it also shows that mannan affects the molecules on MDC but not those on VSV-E1E2.

Discussion

Using the pseudotype VSV system, we have demonstrated that each DC subset has distinct susceptibility to HCV. First, VSV-E1E2 enters MDC but not PDC, which is in sharp contrast with PDC susceptibility to HIV (Patterson et al., 2001). Second, MDC cultured with GM-CSF are more susceptible to VSV-E1E2 than freshly prepared MDC or those cultured with GM-CSF and IL-4, showing that HCV targets immature MDC. Third, certain molecules containing the lectin domain on MDC are involved in the interaction with VSV-E1E2.

One of the suggested mechanisms of persistent HCV infection is the functional suppression of immunocompetent cells, including NK cells, T cells, and DC (Bain et al., 2001; Corado et al., 1997; Kanto et al., 1999; Wedemeyer et al., 2002). The possibility being raised for such immunological impairment is that HCV directly infects these blood cells. To elucidate this issue, investigators have used RT-PCR to examine whether the HCV genome is detectable or not in blood cells recovered from HCV-infected patients (Bain et al., 2001; Lerat et al., 1996, 1998). However, the existence of HCV-RNA does not enable to define whether HCV enters cells or only adheres to their surface. Instead of qualitative RT-PCR, we used the pseudotype VSV system to study the HCV E1E2-mediated virus entry to each DC subset. The pseudotype VSV system is a valid model for investigating the early steps of HCV infection, that is, viral attachment, receptor binding, and membrane fusion. Also, it enables us to estimate the efficiency of HCV E1E2-mediated virus entry to target cells. However, there are several limitations in this system. First, the positive results with pseudotype VSV do not indicate the replicative ability of HCV in the relevant cells. Because pseudotype VSV is constructed from VSV genome, their replication capacity is not exactly the same as HCV. Second, the evaluation of pseudotype VSV entry is possible only in cells that permit VSV replication. In other words, it cannot be used to determine the entry of VSV-E1E2 in the cells that suppress VSV replication. In this study, we could not evaluate the susceptibility of T, B, NK cells or fresh PDC to VSV-E1E2.

Alternatively, we performed an inoculation experiment with authentic HCV particle to confirm the reliability of the pseudotype VSV system. Quantitative RT-PCR assay showed that the highest titer of HCV-RNA was detected in MDC cultured with GM-CSF; however, low titer of HCV-RNA was detected in PDC. We hypothesized that the reason such discrepancy occurs between two assays is that RT-PCR amplified HCV genome from HCV attached to the surface of PDC. Strand-specific RT-PCR showed that negative strand of HCV-RNA, a surrogate marker of HCV replication, was detected in MDC cultured with GM-CSF but not in PDC. These results indicate that HCV enters and replicates in MDC but not in PDC, which are well correlated with those of pseudotype VSV entry.

The Th1 response is thought to be needed to eradicate HCV from hosts (Gerlach et al., 1999). Myeloid DC potentially activate CD4+T cells to support Th1 differentiation (Liu, 2001). We found that MDC from HCV-infected patients are less able to induce the Th1 response than the normal counterpart (Kanto T., unpublished data). It has been reported that MoDC expressing HCV protein were impaired in the stimulation of allogeneic T cells and IL-12 production, indicating an inhibitory capacity of HCV

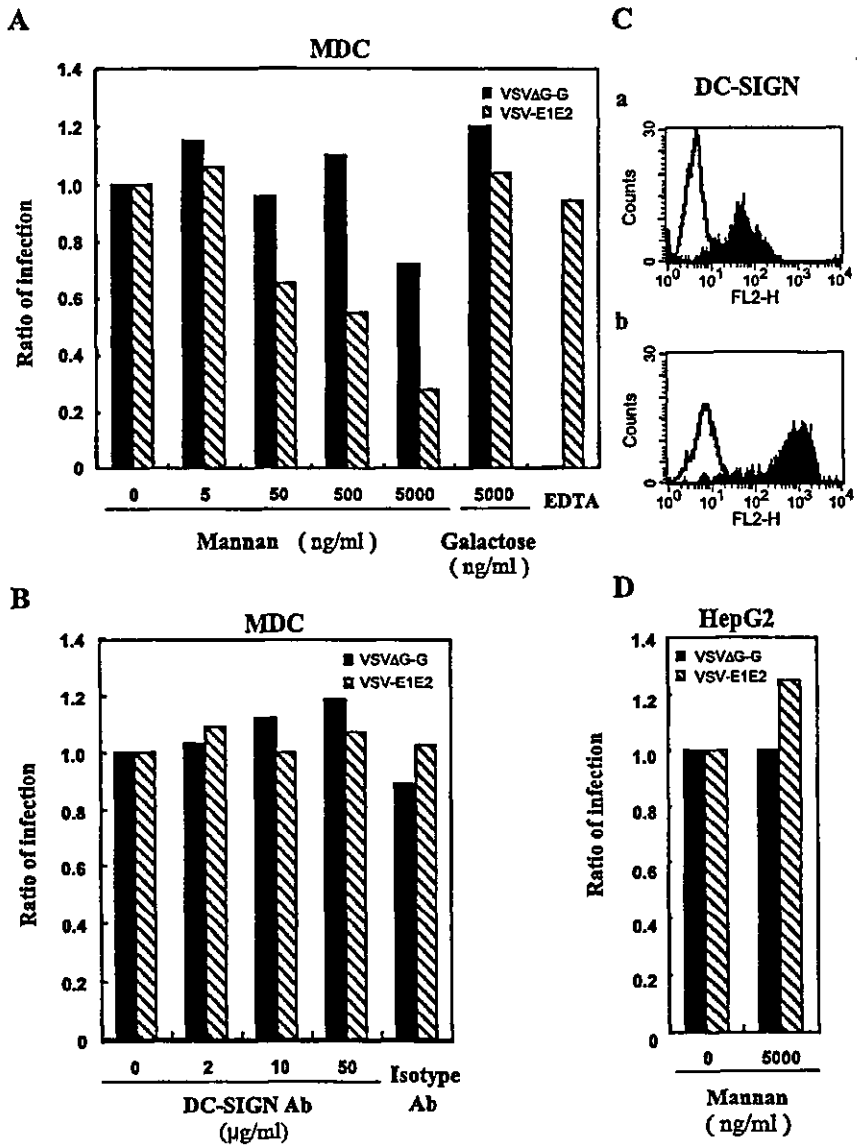

Fig. 5. Mannan inhibits VSV-E1E2 entry to MDC, but not to HepG2. Various concentrations of mannan, galactose, or 5 mM EDTA were added to day 4 MDC cultured with GM-CSF before the pseudotype VSV inoculation. Alternatively, day 4 MDC were treated with 2, 10, or 50 μg/ml antihuman DC-SIGN Ab or 10 μg/ml isotype IgG_{2B} for 30 min before the pseudotype VSV inoculation. HepG2 was treated with 5 μg/ml mannan before the addition of pseudotype VSV. The ratio of infection with pseudotype VSV in MDC (A, B) or HepG2 (D) was determined as described in Materials and method. Representative results are shown from three independent experiments. (C) Flow cytometric analyses were done for DC-SIGN expression on day 4 MDC cultured with GM-CSF (a) or with GM-CSF and IL-4 (b) generated from a healthy volunteer. Representative results from three subjects are shown. Open histograms represent the results with isotype Ab and filled ones represent those with anti-DC-SIGN Abs. Fluorescence intensity is shown in the *x*-axis and the number of cells is shown in the *y*-axis.

protein on DC function (Sarobe et al., 2002). These data suggest that direct HCV infection to myeloid DC suppress their function. Thus, the protection of DC from HCV infection is a rational approach to improve DC-mediated anti-HCV immune response. In the present study, we demonstrate that some of the maturation stimuli are capable of protecting DC from VSV-E1E2 entry. However, MoDC from HCV-infected patients are reported to be resistant to maturation stimuli, such as TNF-α (Auffermann-Gretzinger et al., 2001). Thus, further investigation is necessary to determine the effective modulation that allows MDC to mature in HCV infection. As shown in this study, CpG ODN or CD40L stimulated MDC to mature and become less susceptible to VSV-E1E2. The potent ability of CpG ODN to stimulate a DC-inducing Th1 response has been demonstrated in vivo tumor treatment models (Heckelsmiller et al., 2002). Therefore, CpG ODN are promising as a DC adjuvant in HCV-infected patients that potentially leads to MDC maturation as well as boosting Th1 response.

It is arguably necessary to identify molecules that are responsible for HCV entry to protect DC. Previously, tetraspanin CD81 has drawn much attention as a presumed HCV receptor due to its high affinity to HCV-E2 (Pileri et al., 1998). However, its involvement in VSV-E1E2 entry is unlikely because the CD81 is equally expressed on both MDC and PDC but is lacking on the VSV-E1E2-sensitive cell line HepG2 (Flint et al., 1999). In this study, we showed some of the characteristics of the molecules on DC involved in VSV-E1E2 entry. They are myeloid-lineage specific, inducible by GM-CSF, down-regulatable by IL-4 or other maturation stimuli. In addition, they possess some lectin domain, as evidenced by the inhibition of VSV-E1E2 as well as authentic HCV entry with mannan. These results raised the possibility that such molecules are categorized as members of C-type lectins, such as DC-SIGN, mannose receptor (MR), Langerin, DEC205, BDCA2, or asialoglycoprotein receptor. (Figdor et al., 2002) Recently, two independent studies have demonstrated that HCV E1 and E2 glycoproteins efficiently bind to DC-SIGN (Lozach et al., 2003; Pohlmann et al., 2003). However, the involvement of DC-SIGN in VSV-E1E2 entry is less likely because its expression on MDC did not parallel the susceptibility to VSV-E1E2. In addition, the treatment with anti-DC-SIGN Ab did not inhibit VSV-E1E2 entry. Furthermore, the treatment with EDTA failed to block VSV-E1E2 entry to MDC, showing that the VSV-E1E2 entry occurs in a Ca^{2+}-independent manner. It is still obscure in which step lectins are involved in VSV-E1E2 entry to MDC. From an analogy with the interaction of HIV with DC-SIGN (Geijtenbeek et al., 2000), it is conceivable that lectins are essential for HCV attachment to MDC. Nevertheless, the possibility remains that HCV entry receptors or co-receptors, which may be other than lectins, exist on MDC. With the aid of the pseudotype VSV system, exploration has been underway to identify the molecules on MDC that are critically involved in HCV infection.

Materials and method

Reagents

Recombinant human IL-4 and GM-CSF were purchased from PeproTech (London, UK). Recombinant human soluble CD40L, human TNF-α and IL-3, and mouse monoclonal antihuman DC-SIGN (CD209/DC-SIGN1) Ab (12507) were from R & D Systems (Minneapolis, MN). LPS, polyI:C, mannan, galactose, and methyl α-D-mannnopyranoside were from Sigma (St. Louis, MO). Recombinant human IFN-γ was from Strathman Biotech GmbH (Hamburg, Germany). Human lymphoblastoid IFN-α was provided by Sumitomo Pharmaceuticals (Osaka, Japan). Unmethylated CpG ODN 2006 (Krug et al., 2001) was synthesized at and purchased from Sigma Genosys (Hokkaido, Japan). Isotype IgG (mouse IgG_{2B}) for the blocking experiments was kindly provided from the JT laboratory (Osaka, Japan).

Separation of DC precursors and other cells from PBMC

After informed consent had been obtained from healthy volunteers, buffy coats were isolated from venous blood drawn from them at the Osaka Red Cross Blood Center (Osaka, Japan). PBMC were collected from buffy coats by Ficoll–Hypaque density-gradient centrifugation. B cells, MDC, and PDC were magnetically isolated by using CD19 microbeads, BDCA-1, or BDCA-4 DC isolation kits from Miltenyi Biotec (Bergish-Gladbach, Germany), respectively. BDCA-1^+ and BDCA-4^+ cells are phenotypically compatible with MDC and PDC, respectively (Dzionek et al., 2000). CD4, CD8 T cells, and NK cells were separated from PBMC by using the relevant Stem-Sep kits (Stem Cell Technologies Inc, Vancouver, BC). $CD34^+$ hematopoietic precursor cells were isolated from cord blood mononuclear cells by using CD34-microbeads from Miltenyi. The purity of all isolated cells was more than 90% as determined by FACS Caliber (Becton Dickinson Immunocytometry Systems, San Jose, CA).

Culture of DC

Isolated MDC were cultured for 4 days in IMDM (GIBCO Laboratories, Grand Island, NY) supplemented with 10% FCS, 50 IU/ml penicillin, 50 μg/ml streptomycin, 2 mM L-glutamine, 10 mM Hepes buffer, and 10 μM nonessential amino acid (Complete medium, CM) containing 50 ng/ml GM-CSF with or without 10 ng/ml IL-4. PDC were cultured for 4 days in CM in the presence of 50 ng/ml of IL-3.

Flow cytometry

The expression of surface molecules on DC was analyzed by FACS Caliber (Becton Dickinson). For the staining, DC were stored with specific Abs or isotype Abs for 30 min at 4 °C in PBS containing 2% of BSA and 0.1% of sodium azide. The following FITC-, PE-, PerCP-, or PC5-conjugated antihuman mAbs were used: CD1a (NA1/34; DAKO, Glostrup, Denmark), CD11c (KB90; DAKO), CD14 (M5E2; Becton Dickinson), CD40 (5C3; BD Pharmingen, San Diego, CA), CD80 (L307.4; BD Pharmingen), CD83 (HB15a; Immunotech, Marseille, France), CD86 (IT2.2; B70/B7-2, BD Pharmingen), CDw123 (7G3; IL-3 receptorα chain, BD Pharmingen), DC-SIGN (120507; R & D Systems), and HLA-DR (L243; Becton Dickinson).

Assessment of pseudotype VSV entry into cells

To find which blood cells are susceptible to HCV infection, we used pseudotype VSV possessing chimeric HCV E1 and E2 protein which was generated as described

previously (Matsuura et al., 2001). The pseudotype VSV consists of recombinant VSV in which glycoprotein (G) gene is replaced with a reporter gene encoding GFP.

As an envelope, it possesses chimeric HCV E1 and E2 proteins (VSV-E1E2). The viruses were purified by centrifugation at 25000 rpm for 2 h at 4 °C in SW28 rotor (Beckman Coulter Inc., Fullerton, CA) through 20% (v/w) and 60% (v/w) discontinuous sucrose gradient and were stored at −80 °C. To determine RNA copy numbers in the viral samples, TaqMan EZ RT-PCR kit (PE Applied Biosystems, Foster City, CA) was used. We used forward and reverse primers (5′-cattattatcattaaaaggctc-3′ and 5′-gatacaaggtcaaatattccg-3′) that amplify a 323-bp segment of the pseudotyped VSV RNA and also used a dual fluorophore-labeled probe 5′-(6-carboxy-fluorescein)-atccagtggaatacccggcagattac-(6-carboxy-tetramethyl-rhodamine)-3′. The sequence detector (ABI Prism 7000, PE Applied Biosystems) allows measurement of the amplified products in indirect proportion to the increase in fluorescence emission continuously during the PCR amplification. The copy numbers in samples were determined based on the standard curve drawn by a known amount of in vitro synthesized pseudotyped VSV RNA. Because VSV efficiently replicates in a wide range of mammalian cells, we are able to determine the cells exhibiting susceptibility to pseudotype VSV by the expression of GFP. We used VSV ΔG which has no envelope protein as a negative control. Similarly, VSV ΔG-G was used as a positive control which is complemented with the VSV G protein. Various separated blood cells were prepared in CM at 5×10^4 cells/well on 96-well culture plates. Next, they were inoculated with the pseudotype viruses, VSV-E1E2 (1×10^{12} RNA copies/well), VSV ΔG (1×10^{12} RNA copies/well), or VSV ΔG-G (1×10^{11} RNA copies/well) and incubated for 16 h at 37 °C. The infected cells (GFP^+ cells) were observed under fluorescence microscopy, and their positive percentages were determined by FACS analysis. The net percentage of infected cells was expressed as % infection = (% of GFP^+ cells with VSV-E1E2 or VSV ΔG-G) − (% of GFP^+ cells with VSV ΔG).

To find the substances which potentially protect DC from HCV infection, we examined IFNα, IFNγ, IL-3, IL-4, CpG ODN 2006, CD40L, polyI:C, TNFα, or LPS for this purpose. The appropriate concentrations of these reagents were determined in a separate series of experiments. IFNα, IFNγ, IL-3, or IL-4 was added to DC on the day of separation. CpG ODN 2006, CD40L, polyI:C, TNFα, or LPS was added to DC 24 h before the inoculation of pseudovirus. To compare the inhibitory effect of reagents in VSV-E1E2 entry into cells, we determined the ratio of infection of cells with and without treatment.

DC express various molecules containing the lectin domain, some of which are reported to be essential for the attachment to virus (Figdor et al., 2002). To examine whether lectin-containing molecules on DC are involved in HCV infection, we tested mannan, methyl α-D-mannopyranoside, and galactose for the inhibition of VSV-E1E2 entry. Day 4 MDC cultured with GM-CSF were preincubated with various concentrations of mannan, methyl α-D-mannopyranoside, or galactose at 37 °C for 180 min and inoculated with the pseudotype VSV. We also treated DC with EDTA (5 mM), monoclonal antihuman DC-SIGN Ab (50, 10, or 2 μg/ml), or isotype IgG_{2B} before the pseudotype VSV inoculation. To compare DC with hepatoblastoma cell line, HepG2, we treated HepG2 with mannan before the inoculation.

Quantitative analysis of HCV RNA in cells inoculated with HCV particles from patient serum

To test the susceptibility of each DC subset to authentic HCV, we quantified HCV RNA in cells that had been inoculated with patient serum by means of real-time PCR. We used the commercial HCV seroconversion panel as an inoculum, which contains high HCV RNA titer (1×10^5 copies/μl) and no anti-HCV antibody (BioClinical Partners, Inc, USA). We added 3 μl/well of inoculum to DC on 96-well plates and incubated them at 37 °C for 24 h. DC were harvested and washed three times with IMDM supplemented with 1% FCS and then total RNA was extracted from DC using RNeasy Mini Kit (QIAGEN, Germany). To measure HCV RNA, TaqMan EZ RT-PCR kit (PE Applied Biosystems) was used. We used forward and reverse primers [5′-cgggagagccatagtgg-3′ (positions 130–146) and 5′-agtaccacaaggcctttcg-3′ (positions to 272 to 290)] that amplify a 161-bp segment of the 5′ noncoding region of HCV RNA and also used a dual fluorophore-labeled probe [5′-(6-carboxy-fluorescein)-ctgcggaaccggtgagtacac (positions 148–168)- (6-carboxy-tetramethyl-rhodamine) -3′]. The sequence detector (ABI Prism 7000) allows measurement of the amplified products in indirect proportion to the increase in fluorescence emission continuously during the PCR amplification. The copy number in the samples was determined based on the standard curve drawn by a known amount of in vitro synthesized HCV RNA.

The strand-specific RT-PCR assay for HCV-RNA in cells inoculated with authentic HCV particles

To detect negative-strand HCV-RNA that is indicative of RNA replication, we performed the strand-specific RT-PCR assay referring to the methods described by Navas et al. (2002) with some modifications. We used the same batch of HCV seroconversion panel as an inoculum as described in the above section. We added 3 μl/well of inoculum to DC on 96-well plates and incubated them at 37 °C for 24 h. After the washing of DC for three times, total RNA was extracted from DC as the same way as we did in quantitative RT-PCR. As a control for the detection of HCV-RNA, 9 μl of inoculum was used. We used sense and anti-sense primers [5′-cactcccctgtgaggaactactgtc-3′ (positions 38–62) and 5′-atggtgcacggtctacgagacctcc-3′ (positions 319–343) that amplify a 306-bp segment of the 5′ noncoding region of HCV

genome. Ten microliters of purified RNA was used for reverse transcription (RT) with 10 μl of RT reaction mixture containing the thermostable recombinant *Thermus thermophilus* (rTth) enzyme (PE Applied Biosystems). Synthesis of cDNA was carried out with strand-specific primers, sense primer was used to obtain negative-strand RNA, and antisense primer was used to obtain positive-strand RNA, respectively. Reverse transcription was carried out at 70 °C for 15 min. Subsequently, the same primers were used in reverse order in the PCR rounds. Thirty-five cycles of PCR (94 °C for 45 s, 60 °C for 45 s, 72 °C for 45 s) followed by 7 min of extension at 72 °C were carried out on GeneAmp PCR System (PE Applied Biosystems). One-fifth of the PCR products was subjected to electrophoresis on 2% agarose gel and stained with ethidium bromide for observation under UV light. The expected molecular size of PCR products derived from target HCV RNA was 306 bp.

Statistical analysis

The paired *t* test was used to test the significance of the pseudotype VSV entry to MDC. Statistical analyses were performed with the Statview version 4.5 software (Abacus Concepts, Berkeley, CA). A *P* value of less than 0.05 was considered statistically significant.

Acknowledgment

We are grateful to Dr. Keiji Ueda (Osaka University) for providing cord blood cells.

References

Alter, H.J., Purcell, R.H., Shih, J.W., Melpolder, J.C., Houghton, M., Choo, Q.L., Kuo, G., 1989. Detection of antibody to hepatitis C virus in prospectively followed transfusion recipients with acute and chronic non-A, non-B hepatitis. N. Engl. J. Med. 321 (22), 1494–1500.

Auffermann-Gretzinger, S., Keeffe, E.B., Levy, S., 2001. Impaired dendritic cell maturation in patients with chronic, but not resolved, hepatitis C virus infection. Blood 97 (10), 3171–3176.

Bain, C., Fatmi, A., Zoulim, F., Zarski, J.P., Trepo, C., Inchauspe, G., 2001. Impaired allostimulatory function of dendritic cells in chronic hepatitis C infection. Gastroenterology 120 (2), 512–524.

Banchereau, J., Steinman, R.M., 1998. Dendritic cells and the control of immunity. Nature 392 (6673), 245–252.

Corado, J., Toro, F., Rivera, H., Bianco, N.E., Deibis, L., De Sanctis, J.B., 1997. Impairment of natural killer (NK) cytotoxic activity in hepatitis C virus (HCV) infection. Clin. Exp. Immunol. 109 (3), 451–457.

Dzionek, A., Fuchs, A., Schmidt, P., Cremer, S., Zysk, M., Miltenyi, S., Buck, D.W., Schmitz, J., 2000. BDCA-2, BDCA-3, and BDCA-4: three markers for distinct subsets of dendritic cells in human peripheral blood. J. Immunol. 165 (11), 6037–6046.

Farci, P., Alter, H.J., Govindarajan, S., Wong, D.C., Engle, R., Lesniewski, R.R., Mushahwar, I.K., Desai, S.M., Miller, R.H., Ogata, N., et al., 1992. Lack of protective immunity against reinfection with hepatitis C virus. Science 258 (5079), 135–140.

Figdor, C.G., van Kooyk, Y., Adema, G.J., 2002. C-type lectin receptors on dendritic cells and Langerhans cells. Nat. Rev., Immunol. 2 (2), 77–84.

Flint, M., Thomas, J.M., Maidens, C.M., Shotton, C., Levy, S., Barclay, W.S., McKeating, J.A., 1999. Functional analysis of cell surface-expressed hepatitis C virus E2 glycoprotein. J. Virol. 73 (8), 6782–6790.

Geijtenbeek, T.B., Kwon, D.S., Torensma, R., van Vliet, S.J., van Duijnhoven, G.C., Middel, J., Cornelissen, I.L., Nottet, H.S., KewalRamani, V.N., Littman, D.R., Figdor, C.G., van Kooyk, Y., 2000. DC-SIGN, a dendritic cell-specific HIV-1-binding protein that enhances trans-infection of T cells. Cell 100 (5), 587–597.

Gerlach, J.T., Diepolder, H.M., Jung, M.C., Gruener, N.H., Schraut, W.W., Zachoval, R., Hoffmann, R., Schirren, C.A., Santantonio, T., Pape, G.R., 1999. Recurrence of hepatitis C virus after loss of virus-specific CD4(+) T-cell response in acute hepatitis C. Gastroenterology 117 (4), 933–941.

Grosjean, I., Caux, C., Bella, C., Berger, I., Wild, F., Banchereau, J., Kaiserlian, D., 1997. Measles virus infects human dendritic cells and blocks their allostimulatory properties for CD4+ T cells. J. Exp. Med. 186 (6), 801–812.

Hart, D.N., 1997. Dendritic cells: unique leukocyte populations which control the primary immune response. Blood 90 (9), 3245–3287.

Heckelsmiller, K., Beck, S., Rall, K., Sipos, B., Schlamp, A., Tuma, E., Rothenfusser, S., Endres, S., Hartmann, G., 2002. Combined dendritic cell- and CpG oligonucleotide-based immune therapy cures large murine tumors that resist chemotherapy. Eur. J. Immunol. 32 (11), 3235–3245.

Kaku, H., Goldstein, I.J., Oscarson, S., 1991. Interactions of five D-mannose-specific lectins with a series of synthetic branched trisaccharides. Carbohydr. Res. 213, 109–116.

Kanto, T., Hayashi, N., Takehara, T., Tatsumi, T., Kuzushita, N., Ito, A., Sasaki, Y., Kasahara, A., Hori, M., 1999. Impaired allostimulatory capacity of peripheral blood dendritic cells recovered from hepatitis C virus-infected individuals. J. Immunol. 162 (9), 5584–5591.

Krug, A., Rothenfusser, S., Hornung, V., Jahrsdorfer, B., Blackwell, S., Ballas, Z.K., Endres, S., Krieg, A.M., Hartmann, G., 2001. Identification of CpG oligonucleotide sequences with high induction of IFN-alpha/beta in plasmacytoid dendritic cells. Eur. J. Immunol. 31 (7), 2154–2163.

Lerat, H., Berby, F., Trabaud, M.A., Vidalin, O., Major, M., Trepo, C., Inchauspe, G., 1996. Specific detection of hepatitis C virus minus strand RNA in hematopoietic cells. J. Clin. Invest. 97 (3), 845–851.

Lerat, H., Rumin, S., Habersetzer, F., Berby, F., Trabaud, M.A., Trepo, C., Inchauspe, G., 1998. In vivo tropism of hepatitis C virus genomic sequences in hematopoietic cells: influence of viral load, viral genotype, and cell phenotype. Blood 91 (10), 3841–3849.

Liu, Y.J., 2001. Dendritic cell subsets and lineages, and their functions in innate and adaptive immunity. Cell 106 (3), 259–262.

Lozach, P.Y., Lortat-Jacob, H., de Lacroix de Lavalette, A., Staropoli, I., Foung, S., Amara, A., Houles, C., Fieschi, F., Schwartz, O., Virelizier, J.L., Arenzana-Seisdedos, F., Altmeyer, R., 2003. DC-SIGN and L-SIGN are high affinity binding receptors for hepatitis C virus glycoprotein E2. J. Biol. Chem. 278 (22), 20358–20366.

Matsuura, Y., Tani, H., Suzuki, K., Kimura-Someya, T., Suzuki, R., Aizaki, H., Ishii, K., Moriishi, K., Robison, C.S., Whitt, M.A., Miyamura, T., 2001. Characterization of pseudotype VSV possessing HCV envelope proteins. Virology 286 (2), 263–275.

Miller, R.H., Purcell, R.H., 1990. Hepatitis C virus shares amino acid sequence similarity with pestiviruses and flaviviruses as well as members of two plant virus supergroups. Proc. Natl. Acad. Sci. U.S.A. 87 (6), 2057–2061.

Navas, M.C., Fuchs, A., Schvoerer, E., Bohbot, A., Aubertin, A.M., Stoll-Keller, F., 2002. Dendritic cell susceptibility to hepatitis C virus genotype 1 infection. J. Med. Virol. 67 (2), 152–161.

Patterson, S., Rae, A., Hockey, N., Gilmour, J., Gotch, F., 2001. Plasmacytoid dendritic cells are highly susceptible to human immunodeficiency virus type 1 infection and release infectious virus. J. Virol. 75 (14), 6710–6713.

Pileri, P., Uematsu, Y., Campagnoli, S., Galli, G., Falugi, F., Petracca, R.,